the interaction between nonviral gene vectors and biological components has not been reported due to the absence of methodology to quantify the interaction. We recently described a method of direct and instantaneous observation of intravenously injected substances using intravital real-time confocal laser scanning microscopy (IVRTCLSM) [9]. IVRTCLSM provides high-speed scanning and simultaneous capture of multicolor fluorescence. The macromolecular agents flowing in the bloodstream in tumors, kidneys, and livers can be monitored using IVRTCLSM.

In the present study, we applied IVRTCLSM for the investigation of the interaction between nonviral gene vectors and biological components *in situ*. For the PEGylated polyplexes, we focused on polyplex micelles made through the self-assembly of pDNA with PEG-based cationic block copolymers [10–12]. We further developed an analytical methodology to quantify the dynamic states of nonviral gene vectors circulating in the bloodstream. This is the first report visualizing and quantifying the interaction between nonviral gene vectors and biological components over time and in real-time *in situ*.

2. Experimental methods

2.1. Sample preparation

Sterile Hepes (1 M, pH 7.3) was purchased from Amresco (Solon, OH, USA) and used as a buffer solution after dilution with distilled water. pDNA encoding the soluble form of vascular endothelial growth factor receptor-1 was labeled with Cy5 using Label IT Tracker Nucleic Acid Localization Kits (Mirus Bio Corporation, Madison, WI, USA). BPEI (molecular weight (MW) 22 kDa; Sigma-Aldrich, St. Louis, MO, USA) was dialyzed in 0.01 M HCl and lyophilized as a hydrochloride salt. BPEI and PLys (hydrobromide salt, MW 4–15 kDa; Sigma-Aldrich) were mixed with Cy5-labeled pDNA (150 μg/mL) at an N/P ratio of 6 and 2, respectively, to form polyplexes. The N/P ratio was defined as the residual molar ratio of amino groups of cationic segment to phosphate groups of pDNA. Poly{*N*-[*N*-(2-aminoethyl)-2-aminoethyl]aspartamide} (PAsp(DET)) (polymerization degree: 95) was synthesized as described previously [13]. PAsp(DET) was mixed with Cy5-labeled pDNA at an N/P ratio of 4. Poly(ethylene glycol)-*b*-poly(L-lysine) (PEG-PLys; MW of PEG: 12,000; polymerization degree of PLys segment: 45) was synthesized as described previously [14]. Poly(ethylene glycol)-*b*-poly{*N*-[*N*-(2-aminoethyl)-2-aminoethyl]aspartamide} (PEG-PAsp(DET); MW of PEG: 12,000 Da; polymerization degree of PAsp(DET) segment: 93) was synthesized by the aminolysis of PEG-poly(β-benzyl L-aspartate) block copolymer with diethylenetriamine according to a previous report [13]. PEG-PLys/pDNA and PEG-PAsp(DET)/pDNA micelles were prepared at an N/P ratio of 2 and 4, respectively. The final Cy5-labeled pDNA concentration was adjusted to 100 μg/mL in 10 mM Hepes buffer (pH 7.3).

2.2. Animal preparation

All animal experimental procedures were executed in accordance with the Guide for the Care and Use of Laboratory Animals as stated by the National Institutes of Health. Balb/c nude mice (female; Charles River Laboratories, Tokyo, Japan) were anesthetized with 3.0%–4.0% isoflurane (Abbott Japan Co., Ltd., Tokyo, Japan) using a Univenter 400 Anaesthesia Unit (Univentor Ltd., Zejtun, Malta). Mice were then subjected to lateral tail vein catheterization with a 30-gauge needle (Dentronics Co., Ltd., Tokyo, Japan) connected to a nontoxic, medical grade polyethylene tube (Natsume Seisakusho Co., Ltd., Tokyo, Japan). Platelets were labeled *in vivo* with the intravenous injection of DyLight 488-conjugated anti-GPIbβ antibody (X488; EMFRET Analytics, Eibelstadt, Germany) following the manufacturer's instructions. Mice were placed onto a custom-designed temperature-controlled microscope stage. The ear lobe was attached beneath the cover slip with a single drop of immersion oil as described in our previous report [9]. Video acquisition of the dermis tissue at a speed of 30 frames per second was performed for 10 min. Two-hundred microliters of naked pDNA, polyplexes, and micelles (20 μg of pDNA) were administered via the tail vein catheter 10 s after video acquisition was initiated. For the platelet inhibition study, 300 μL of aspirin (acetylsalicylic acid; Sigma-Aldrich) saturated aqueous solution was orally administered to mice for 2 consecutive days before IVRTCLSM.

2.3. IVRTCLSM imaging and processing

All picture/movie acquisitions were performed using a Nikon A1R confocal laser scanning microscope system attached to an upright ECLIPSE FN1 machine equipped with a CFI Apo 40× WI λS objective lens (Nikon, Tokyo, Japan). All pictures/movies were acquired at a scale of 79.55 μm × 79.55 μm with 5.11 μm of confocal slice. Acquired data were further processed using Nikon NIS Elements software. The region of interest (ROI) was manually defined in the vein. Image frames were extracted every 5 s from the video data for further analyses. For quantification of aggregates, the coefficient of variation (CV) of Cy5 fluorescence was calculated. For the platelet interaction study, colocalization between DyLight and Cy5 was evaluated by Pearson's correlation coefficient (PCC) [15]. All obtained values were plotted against time.

3. Discovery

3.1. Real-time observation of aggregates

We prepared BPEI/pDNA (N/P = 6), PLys/pDNA (N/P = 2), and PAsp (DET)/pDNA (N/P = 4) polyplexes as well as PEG-PLys/pDNA (N/P = 2) and PEG-PAsp(DET)/pDNA (N/P = 4) micelles. BPEI/pDNA was used as the representative polyplex containing excessive polycations. N/P ratios of PLys/pDNA and PAsp(DET)/pDNA were determined as the critical ratio to condense pDNA according to our previous report [16]. N/P ratios of PEG-PLys/pDNA and PEG-PAsp(DET)/pDNA micelles were determined at the same N/P ratios of PLys/pDNA and PAsp(DET)/pDNA polyplexes, respectively. The size and zeta potentials of these polyplexes and polyplex micelles were summarized in Supplementary Table 1.

Intravenously injected polyplexes and micelles were directly observed by IVRTCLSM. These dynamic states in the bloodstream were compared (Supplementary Videos 1–5). Extracted movie frames at indicated time points are shown in Fig. 1. Immediately after the BPEI/pDNA polyplex was injected, the fluorescence of Cy5 agglomerated into clumps with a variable size in several micrometers range. This nonuniform fluorescence distribution of the polyplex indicated formation of aggregates. PLys/pDNA and PAsp(DET)/pDNA polyplexes showed similar aggregate formation. In contrast, the fluorescence of Cy5 showed uniform distribution when PEG-PLys/pDNA and PEG-PAsp(DET)/pDNA micelles were injected, indicating the absence of aggregates.

3.2. Quantification of aggregates

Using the mean intensity of Cy5 fluorescence, the amount of Cy5-labeled pDNA was evaluated. We acquired the images every 5 s, calculated the relative fluorescence intensity defined as (Cy5 mean fluorescence intensity - Cy5 minimum fluorescence intensity)/(Cy5 maximum fluorescence intensity − Cy5 minimum fluorescence intensity), and plotted the relative fluorescence intensities against time. (Supplementary Fig. 1) The relative fluorescence intensities of naked pDNA decreased immediately, and almost disappeared within 5 min after the start of acquisition. The relative fluorescence intensities of BPEI/pDNA, PLys/pDNA, and PAsp(DET)/pDNA polyplexes also rapidly decreased and dropped to around 0.2 within 10 min after the start of acquisition. In contrast, PEG-PLys/pDNA, and PEG-PAsp(DET)/pDNA polyplex micelles maintained the relative

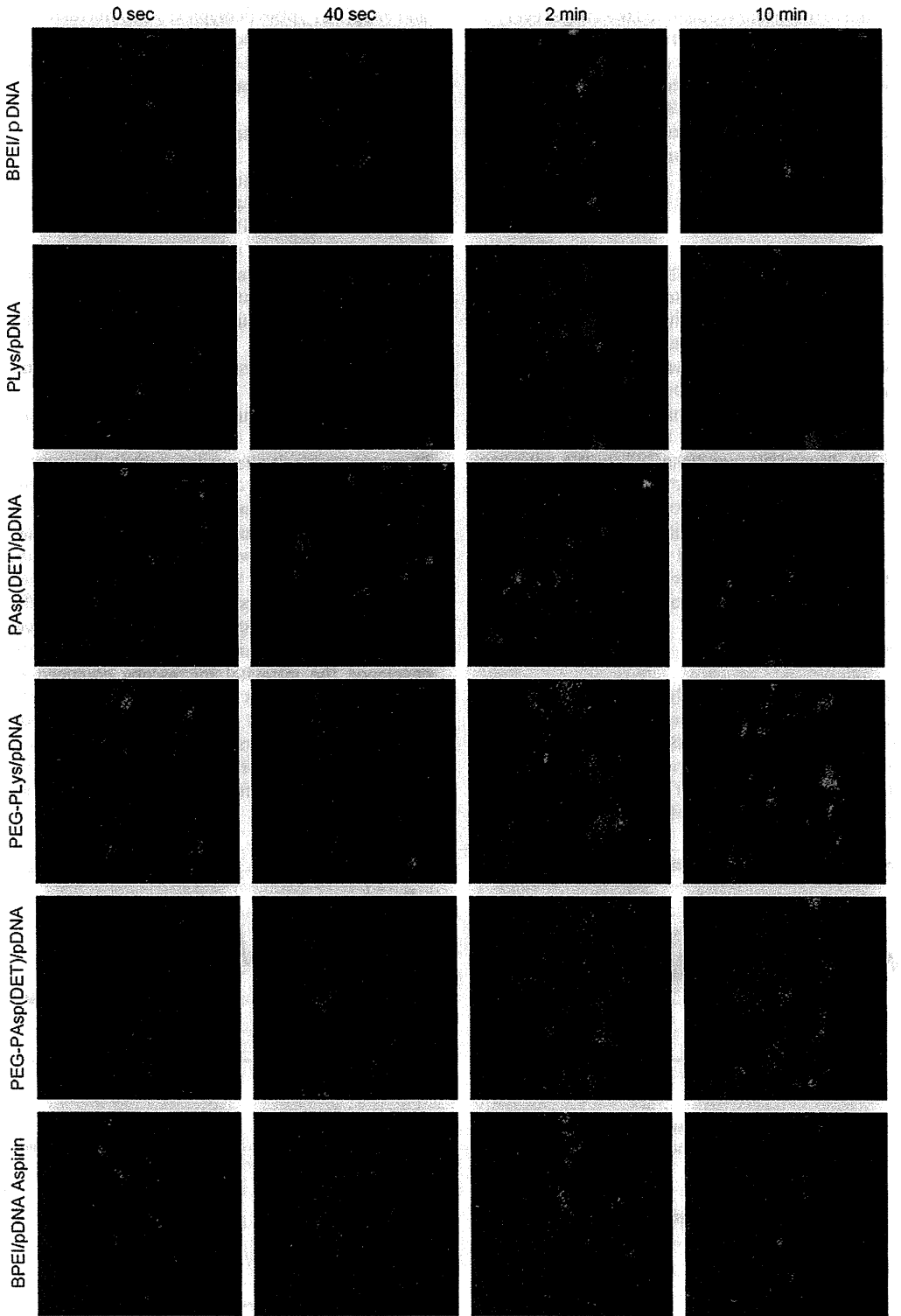

Fig. 1. Intravital confocal micro-videography of polyplexes and polyplex micelles in the bloodstream of the mouse earlobe. Prior to observation, the anti-GPIbβ antibody conjugated with DyLight 488 was injected to label platelets (green). The polyplexes and polyplex micelles incorporating Cy5-labeled pDNA (red) were intravenously injected 10 s after start of observation. Image frames were extracted from videos at identical time points for comparison. Image size: 79.55 μm × 79.55 μm. Confocal slice: 5.11 μm.

fluorescence intensities of around 0.9 and 0.7 even 10 min after the start of acquisition, suggesting the prolonged blood circulation. These results are consistent with the previous studies, which demonstrated pDNA degradation within 5 min and the improvement of blood circulation by PEGylation [17,18].

However, the relative fluorescence intensities could not provide the information about the aggregates of polyplexes and polyplex micelles. Thus, the quantification of aggregates was performed by CV calculation of Cy5 fluorescence in the ROI. The CV is a normalized measure of dispersion of a distribution, and is defined as the ratio of

the standard deviation to the mean. We acquired the images every 5 s, calculated the CV, and plotted the CV against time (Fig. 2). CV values of the polyplexes rapidly increased upon first entry into the vein of the earlobe immediately after intravenous injection. CV values of the polyplexes subsequently fluctuated and decreased over time. In contrast, CV values of the micelles slightly increased upon first entry due to the admixture of micelles and blood, and remained at a plateau at the lower values without fluctuation.

3.3. Platelet interaction study

Platelet is known to be the primary cell components involved in the initial event of thrombosis, and polycations initiate the process of platelet clots formation [19–21]. Thus, in this study, we focused on platelets interaction with cationic polyplexes. To investigate the interaction of polyplexes with platelets, we labeled platelets with DyLight 488-conjugated anti-GPIbβ antibody, and observed the interaction using IVRTCLSM (Fig. 1, Supplementary Videos 1–5). The average labeling efficiency of the antibody has been reported to be ~90% [22]. BPEI/pDNA, PLys/pDNA, and PAsp(DET)/pDNA polyplexes formed aggregates immediately after injection as described above. Their adhesion to platelets was clearly observed approximately 2 min after injection as judged from the colocalization of red and green fluorescences to appear as yellow colored pixels. In contrast, PEG-PLys/pDNA and PEG-PAsp(DET)/pDNA micelles showed no adhesion to platelets throughout the whole experiment.

3.4. Platelet interaction quantification

To quantify the interaction between polyplexes and platelets, we acquired the images every 5 s, and calculated the colocalization between Cy5 fluorescence and DyLight 488 fluorescence using PCC [15]. PCC indicates the intensity of the correlation of two elements, ranging from −1 to +1. The PCC value of the BPEI/pDNA polyplex fluctuated and increased up to approximately 0.4 (Fig. 3). PLys/pDNA and PAsp(DET)/pDNA polyplexes also fluctuated and increased up to approximately 0.25 and 0.33, respectively. In contrast, PCC values of PEG-PLys/pDNA and PEG-PAsp(DET)/pDNA micelles were maintained at almost zero throughout the study.

3.5. Platelet inhibition study

To investigate whether inhibition of platelet function decreases aggregates formation, aspirin was used as an anti-platelet agent. We compared the CV and PCC of the BPEI/pDNA polyplex between aspirin-administered mice and nonadministered control mice (Figs. 1 and 4, Supplementary Video 6). The CV value of the aspirin-administered mice was almost identical to that of control mice; however, their PCC value remained <0.1 throughout the study.

4. Interpretation and significance of new methodologies

Pharmacokinetic studies are indispensable for developing efficient DDSs that transport drugs specifically to the targeted tissue. Pharmacokinetic studies using animals have primarily relied on *ex vivo* techniques, such as analyzing blood or urine samples. These *ex vivo* techniques have been well established to analyze blood circulation, target accumulation, or other pharmacological information of the DDS. However, this approach provides only static information at specific time points. Therefore, investigating dynamic and longitudinal events using this approach is difficult. Alternatively, the intravital microscopy is an emerging technique [23], allowing to investigate such dynamic states of DDS in animals. Recently, we developed the intravital microscopy equipped with fast-scanning laser confocal systems (IVRTCLSM) [9], and demonstrated here its application as a novel tool to dynamically evaluate the interaction between gene vectors and blood components. Our method is characterized by noninvasive observation with high spatial and temporal resolutions to quantitatively monitor the dynamic states

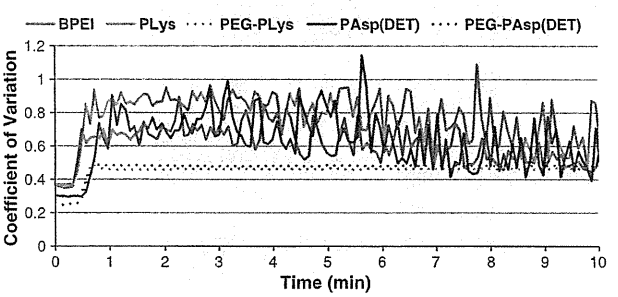

Fig. 2. Quantification of aggregates of polyplexes and micelles. Aggregates of polyplexes and micelles were quantified with CV of Cy5 fluorescence intensities in the frames extracted every 5 s from crude videos.

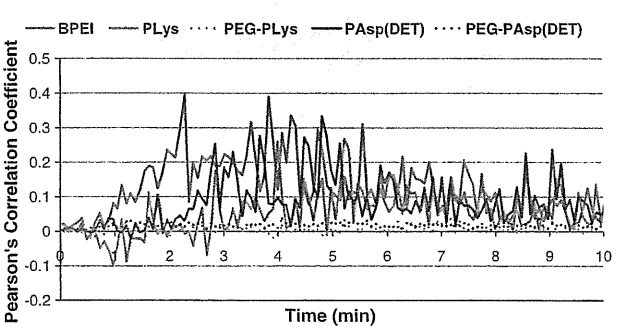

Fig. 3. Quantification of colocalization between polyplexes/micelles and platelets. The colocalization was measured with PCC. PCC was calculated from the frames extracted every 5 s from crude videos.

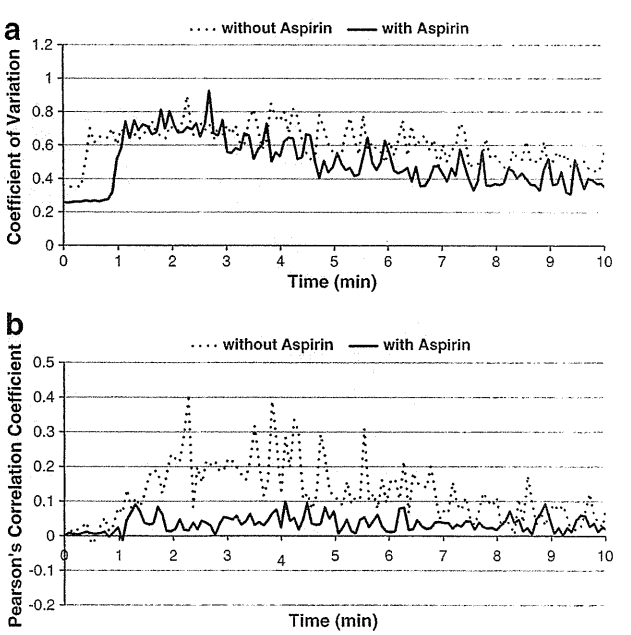

Fig. 4. Platelets inhibition study with aspirin. (a) Aggregates of BPEI/pDNA polyplexes of the aspirin-administered mouse was quantified with the CV of Cy5 fluorescence intensities in the frames extracted every 5 s from crude videos. (b) Colocalization between BPEI/pDNA polyplexes and platelets of the aspirin-administered mouse was quantified with PCC. PCC was calculated from the frames extracted every 5 s from crude videos. For comparison, the CV and PCC of the BPEI/pDNA polyplexes-administered normal mouse in Figs. 2 and 3 were shown respectively again.

of nonviral gene vectors. In the present study, the mouse earlobe was noninvasively fixed beneath the coverslip, and the vein was imaged at the dermis layer. Confocal imaging eliminated light from out-of-focus sections in the ear lobe such as the epidermis and hypodermis. Furthermore, we kept the confocal slice thinner (5.11 μm) than the diameter of the vein, so that the signal was detected only from inside the vasculature. High-speed scanning was essential to obtain unambiguous images to quantify the aggregates and colocalization between nonviral gene vectors and platelets because conventional galvano scanners are too slow to distinguish the individual aggregates and platelets rapidly flowing in the bloodstream, providing insufficient and blurred images (Supplementary Videos 7 and 8).

We investigated the polycations BPEI and PLys. They are widely used to construct polyplexes and PAsp(DET) has reduced cytotoxicity and high transfection efficiency [13]. To evaluate the improvement of biocompatibility via PEGylation, PEG-PLys/pDNA and PEG-PAsp (DET)/pDNA micelles were examined. A simple and effective way to PEGylate polyplexes is, as we reported [10–12], to use PEG-based cationic block copolymers as counterpart polycations to pDNA. The block copolymers are characterized by tandem alignment of a hydrophilic PEG segment and a cationic segment, leading to the formation of stable and biocompatible micelles with a core of polycation/pDNA complex surrounded by a dense PEG palisade and size of approximately 100 nm. Indeed, the micelle composed of PEG-PLys and pDNA achieved higher stability than that of unmodified PLys/pDNA polyplex in a medium containing serum and showed prolonged blood circulation [18,24]. The block copolymer possessing a cationic polyaspartamide segment carrying an ethylenediamine unit at the side chain, PEG-PAsp(DET), also formed the micelle with pDNA, which prevented nonspecific interaction with biological components such as erythrocytes and platelets under *in vitro* conditions [8].

IVRTCLSM was used to directly investigate the interaction between these gene vectors and platelets in the bloodstream. IVRTCLSM could be used to evaluate the dynamic states of nonviral gene vectors rapidly flowing in the bloodstream over time *in situ* (Fig. 1 and Supplementary Videos 1–6). This is the first report to visualize the formation of aggregates and the prevention by PEGlyation of polyplexes *in situ* in the bloodstream.

To quantify the aggregates, we adopted the CV. CV values reflected the nonuniform fluorescence distribution of polyplexes and uniform fluorescence distribution of micelles (Fig. 2). It is noteworthy that our IVRTCLSM started video acquisition 10 s before administration, allowing us to follow aggregate formation immediately after injection. CV values of the polyplexes rapidly increased approximately 20–30 s after injection, and corresponded well with the entry of polyplexes, indicating instantaneous formation of aggregates (Fig. 2). CV values also fluctuated over time, depending on the amount of aggregates at those time points. Furthermore, CV values of polyplexes decreased with time due to their disappearance from the bloodstream. In contrast, CV values of micelles were moderately elevated when micelles passed the ROI first. This moderate elevation was because of the admixture of micelles and blood without aggregate formation. Moreover, CV values were retained at a plateau after this moderate elevation, suggesting persistent circulation and uniform distribution of micelles in the bloodstream.

IVRTCLSM was also useful for the investigation of the dynamic interaction between nonviral gene vectors and platelets. Indeed, we succeeded in visualizing the interaction between polyplexes and platelets *in situ*. This dynamic information could not be revealed without IVRTCLSM.

To quantify the platelet interaction, we adopted PCC between polyplexes/micelles and platelets (Fig. 3). PCC values of polyplexes did not increase at the time point when CV values started to increase. PCC values began to increase after approximately 1 min after injection, and indicated strong correlation between polyplexes and platelets 2 min after injection. This temporal gap between aggregate formation and platelet interaction strongly indicated that aggregate formation was not triggered by platelets. To confirm this, we conducted the study in mice that were administered aspirin (Fig. 4). Aspirin induces a long-lasting functional defect in platelets [25], and thus may inhibit platelet interaction with polyplexes. The CV and PCC quantitatively demonstrated that oral administration of aspirin successfully inhibited platelet interaction with aggregates (Fig. 4b), but did not inhibit aggregate formation itself (Fig. 4a). This result indicates that the aggregate formation of polyplexes does not involve platelets (at least in the initial stage). Presumably, some protein components in plasma may have a role in aggregate formation, but further investigation is needed to clarify the mechanism.

Aggregate formation in the range of several micrometers immediately after intravenous injection should crucially affect the efficiency of systemically injected polyplexes. The aggregated polyplexes cannot extravasate into the targeted tissues or cells. Moreover, they might lead to thrombosis through the interaction with platelets to obstruct microvessels in normal tissue, including the lungs and liver, resulting in nonspecific accumulation of polyplexes in these tissues. This accumulation caused by aggregate formation will lead to unfavorable effects such as pulmonary embolism. The micelles, in contrast, did not form aggregates, and also showed no interaction with platelets. Thus, they are expected to prevent adverse effects caused by polyplex agglomeration, which cannot be inhibited even by oral administration of aspirin. This result confirms that PEGylation is a rational strategy to improve the biocompatibility of nonviral gene vectors based on polyplex formation [3,10–12].

In the present study, IVRTCLSM was used to visualize and quantify the dynamic states of polyplexes flowing in the bloodstream. Moreover, with respect to ethics, IVRTCLSM excels conventional *ex vivo* methods that involve the sacrifices of numerous animals to acquire pharmacokinetic information. IVRTCLSM provides temporal and spatial information at 30 time points in 1 s with a single mouse, which is desirable for high-throughput screening of newly developed DDSs.

In conclusion, IVRTCLSM was developed and applied to directly investigate the dynamic state of gene vectors in the bloodstream. Aggregate formation of the polyplexes and its prevention by PEGylation was observed *in situ* for the first time under the flow in the capillary. Thus, IVRTCLSM could provide the requisite information that has not been obtained by conventional methods, thereby giving a new facet in the research on systemic gene delivery.

Supplementary materials related to this article can be found online at doi:10.1016/j.jconrel.2011.02.011.

Acknowledgment

This work was supported in part by Core Research Program for Evolutional Science and Technology (CREST) from the Japan Science and Technology Corporation (JST) and Funding Program for World-Leading Innovative R&D on Science and Technology (FIRST Program) from Japan Society for the Promotion of Science (JSPS).

References

[1] D.W. Pack, A.S. Hoffman, S. Pun, P.S. Stayton, Design and development of polymers for gene delivery, Nat. Rev. Drug Discov. 4 (2005) 581–593.
[2] T. Merdan, K. Kunath, H. Petersen, U. Bakowsky, K.H. Voigt, J. Kopecek, T. Kissel, PEGylation of poly(ethylene imine) affects stability of complexes with plasmid DNA under in vivo conditions in a dose-dependent manner after intravenous injection into mice, Bioconjug. Chem. 16 (2005) 785–792.
[3] M. Ogris, E. Wagner, Targeting tumors with non-viral gene delivery systems, Drug Discov. Today 7 (2002) 479–485.
[4] Y. Kakizawa, K. Kataoka, Block copolymer micelles for delivery of gene and related compounds, Adv Drug Deliver Rev 54 (2002) 203–222.

[5] K. Osada, R.J. Christie, K. Kataoka, Polymeric micelles from poly(ethylene glycol)-poly(amino acid) block copolymer for drug and gene delivery, J. R. Soc. Interface 6 (2009) S325–S339.
[6] Y.Y. Yang, Y. Wang, R. Powell, P. Chan, Polymeric core–shell nanoparticles for therapeutics, Clin. Exp. Pharmacol. Physiol. 33 (2006) 557–562.
[7] M. Ogris, S. Brunner, S. Schuller, R. Kircheis, E. Wagner, PEGylated DNA/transferrin-PEI complexes: reduced interaction with blood components, extended circulation in blood and potential for systemic gene delivery, Gene Ther. 6 (1999) 595–605.
[8] D. Akagi, M. Oba, H. Koyama, N. Nishiyama, S. Fukushima, T. Miyata, H. Nagawa, K. Kataoka, Biocompatible micellar nanovectors achieve efficient gene transfer to vascular lesions without cytotoxicity and thrombus formation, Gene Ther. 14 (2007) 1029–1038.
[9] Y. Matsumoto, T. Nomoto, H. Cabral, Y. Matsumoto, S. Watanabe, R.J. Christie, K. Miyata, M. Oba, T. Ogura, Y. Yamasaki, N. Nishiyama, T. Yamasoba, K. Kataoka, Direct and instantaneous observation of intravenously injected substances using intravital confocal micro-videography, Biomed. Opt. Express 1 (2010) 1209–1216.
[10] K. Osada, R.J. Christie, K. Kataoka, Polymeric micelles from poly(ethylene glycol)-poly(amino acid) block copolymer for drug and gene delivery, J. R. Soc. Interface 6 (Suppl. 3) (2009) S325–339.
[11] Y. Kakizawa, K. Kataoka, Block copolymer micelles for delivery of gene and related compounds, Adv. Drug Deliv. Rev. 54 (2002) 203–222.
[12] N. Nishiyama, K. Kataoka, Current state, achievements, and future prospects of polymeric micelles as nanocarriers for drug and gene delivery, Pharmacol. Ther. 112 (2006) 630–648.
[13] K. Itaka, T. Ishii, Y. Hasegawa, K. Kataoka, Biodegradable polyamino acid-based polycations as safe and effective gene carrier minimizing cumulative toxicity, Biomaterials 31 (2010) 3707–3714.
[14] A. Harada, K. Kataoka, Formation of polyion complex micelles in an aqueous milieu from a pair of oppositely-charged block-copolymers with poly(ethylene glycol) segments, Macromolecules 28 (1995) 5294–5299.
[15] V. Zinchuk, O. Zinchuk, T. Okada, Quantitative colocalization analysis of multicolor confocal immunofluorescence microscopy images: pushing pixels to explore biological phenomena, Acta Histochem. Et Cytochem. 40 (2007) 101–111.
[16] K. Miyata, S. Fukushima, N. Nishiyama, Y. Yamasaki, K. Kataoka, PEG-based block catiomers possessing DNA anchoring and endosomal escaping functions to form polyplex micelles with improved stability and high transfection efficacy, J. Control. Release 122 (2007) 252–260.
[17] K. Kawabata, Y. Takakura, M. Hashida, The fate of plasmid dna after intravenous-injection in mice – involvement of scavenger receptors in its hepatic-uptake, Pharm. Res. 12 (1995) 825–830.
[18] M. Harada-Shiba, K. Yamauchi, A. Harada, I. Takamisawa, K. Shimokado, K. Kataoka, Polyion complex micelles as vectors in gene therapy – pharmacokinetics and in vivo gene transfer, Gene Ther. 9 (2002) 407–414.
[19] K. Kataoka, T. Tsuruta, T. Akaike, Y. Sakurai, Biomedical behavior of synthetic polyion complexes toward blood-platelets, Makromolekulare Chem. Macromol. Chem. Phys. 181 (1980) 1363–1373.
[20] T.K. Rosborough, Parallel inhibition of ristocetin and polycation-induced platelet agglutination, Thromb. Res. 19 (1980) 417–422.
[21] P. Chollet, M.C. Favrot, A. Hurbin, J.L. Coll, Side-effects of a systemic injection of linear polyethylenimine–DNA complexes, J. Gene Med. 4 (2002) 84–91.
[22] M.R. Dowling, E.C. Josefsson, K.J. Henley, P.D. Hodgkin, B.T. Kile, Platelet senescence is regulated by an internal timer, not damage inflicted by hits, Blood 116 (2010) 1776–1778.
[23] S. Hak, N.K. Reitan, O. Haraldseth, C. Lange Davies, Intravital microscopy in window chambers: a unique tool to study tumor angiogenesis and delivery of nanoparticles, Angiogenesis 13 (2010) 113–130.
[24] K. Itaka, K. Yamauchi, A. Harada, K. Nakamura, H. Kawaguchi, K. Kataoka, Polyion complex micelles from plasmid DNA and poly(ethylene glycol)-poly(L-lysine) block copolymer as serum-tolerable polyplex system: physicochemical properties of micelles relevant to gene transfection efficiency, Biomaterials 24 (2003) 4495–4506.
[25] C. Patrono, Aspirin as an antiplatelet drug, N. Engl. J. Med. 330 (1994) 1287–1294.

Journal of Controlled Release 149 (2011) 51–57

Contents lists available at ScienceDirect

Journal of Controlled Release

journal homepage: www.elsevier.com/locate/jconrel

GENE DELIVERY

Antiangiogenic gene therapy of experimental pancreatic tumor by sFlt-1 plasmid DNA carried by RGD-modified crosslinked polyplex micelles

Yelena Vachutinsky [a], Makoto Oba [b], Kanjiro Miyata [c], Shigehiro Hiki [d], Mitsunobu R. Kano [e], Nobuhiro Nishiyama [c,f], Hiroyuki Koyama [b], Kohei Miyazono [e,f], Kazunori Kataoka [a,c,d,f,*]

[a] Department of Bioengineering, Graduate School of Engineering, The University of Tokyo, 7-3-1 Hongo, Bunkyo-ku, Tokyo 113-8656, Japan
[b] Department of Clinical Vascular Regeneration, Graduate School of Medicine, The University of Tokyo, 7-3-1 Hongo, Bunkyo-ku, Tokyo 113-8655, Japan
[c] Center for Disease Biology and Integrative Medicine, Graduate School of Medicine, The University of Tokyo, 7-3-1 Hongo, Bunkyo-ku, Tokyo 113-0033, Japan
[d] Department of Materials Engineering, Graduate School of Engineering, The University of Tokyo, 7-3-1 Hongo, Bunkyo-ku, Tokyo 113-8656, Japan
[e] Department of Molecular Pathology, Graduate School of Medicine, The University of Tokyo, 7-3-1 Hongo, Bunkyo-ku, Tokyo 113-8655, Japan
[f] Center for Nano-Bio Integration The University of Tokyo, 7-3-1 Hongo, Bunkyo-ku, Tokyo 113-8656, Japan

ARTICLE INFO

Article history:
Received 5 October 2009
Accepted 1 February 2010
Available online 6 February 2010

Keywords:
Poly(ethylene glycol)-*block*-poly(L-lysine) (PEG-P(Lys)
Cyclic RGD peptide
sFlt-1
Antiangiogenic gene therapy
Polyplex micelle

ABSTRACT

Disulfide crosslinked polyplex micelles with RGD peptides were formed through ion complexation of thiolated c(RGDfK)-poly(ethylene glycol)-*block*-poly(L-lysine) (c(RGDfK)-PEG-P(Lys-SH)) and plasmid DNA encoding sFlt-1 and tested for their therapeutic effect in BxPC3 pancreatic adenocarcinoma tumor bearing mice. These micelles, systemically injected, demonstrated significant inhibition of tumor growth up to day 18, as a result of the antiangiogenic effect that was confirmed by vascular density measurements. Significant therapeutic activity of the 15% crosslinked micelle (c(RGDfK)-PEG-P(Lys-SH15)) was achieved by combined effect of increased tumor accumulation, interaction with endothelial cells and enhanced intracellular uptake through receptor-mediated endocytosis. These results suggest that RGD targeted crosslinked polyplex micelles can be effective plasmid DNA carriers for antiangiogenic gene therapy.

1. Introduction

Poly(ethylene glycol) (PEG)-polycation block copolymers have been widely investigated in the field of gene delivery as a potential non-viral vectors for systemic applications [1–7]. The complexes of plasmid DNA (pDNA) and block copolymers form self-assembling particles, termed polyplex micelles, with a core-shell structure. The outer hydrophilic shell layer, formed by PEG segment, increases micelle stability in serum, improves its pharmacokinetic properties, and reduces polymer toxicity [8–11]. Nevertheless, further stabilization and increased longevity in blood are required for polyplex micelles to achieve successful gene delivery *in vivo*.

Disulfide crosslinks were previously introduced into the polyplex micelle core to stabilize its structure in the extracellular entity, while facilitating smooth release of the entrapped pDNA in the intracellular reductive environment [12,13]. Indeed, disulfide crosslinked polyplex micelles exhibited improved transfection of the reporter gene to cultured cells and mouse liver upon systemic administration [13]. In addition, cyclic RGD peptide ligands (c(RGDfK)) were recently installed onto the surface of the disulfide crosslinked polyplex micelles to achieve specific targeting to tumor neo-vasculature [14,15]. RGD (Arg–Gly–Asp) peptide is a recognition motif in multiple ligands of α_v integrin family [16]. Moreover, cyclic RGD peptides showed increased affinity to $\alpha_v\beta_3$ and $\alpha_v\beta_5$ integrin receptors [17] which are overexpressed on tumor angiogenic endothelial cells [18]. Therefore, RGD peptide ligands have been intensively investigated as an active targeting strategy in antiangiogenic gene therapy for cancer [19–22]. Consequently, we hypothesized that polyplex micelles with cyclic RGD ligands and disulfide crosslinks may be a useful system for targeting angiogenic endothelial cells by systemic administration. RGD conjugated polyplex micelles showed remarkably increased transfection efficiency in cultured HeLa cells possessing $\alpha_v\beta_3$ and $\alpha_v\beta_5$ integrins, as a result of increased cellular uptake and intracellular trafficking of micelles toward perinuclear region via caveolae-mediated endocytosis as was previously reported [14,15]. Caveolae- mediated endocytosis is a nondigestive internalization pathway, which does not result in pH decrease, thus avoiding pDNA degradation in acidic organelles in cell. This route might be especially essential for polylysine based pDNA carriers, which do not possess "proton buffering" ability to escape endosome.

Vascular endothelial growth factor (VEGF) is a major proangiogenic molecule, which stimulates angiogenesis via promoting endothelial proliferation, survival and migration [reviewed in [23,24]]. VEGF and VEGF receptors have been found to be up-regulated in

* Corresponding author. Department of Bioengineering, Graduate School of Engineering, The University of Tokyo, 7-3-1 Hongo, Bunkyo-ku, Tokyo 113-8656, Japan. Tel.: +81 3 5841 7138; fax: +81 3 5841 7139.
E-mail address: kataoka@bmw.t.u-tokyo.ac.jp (K. Kataoka).

0168-3659/$ – see front matter © 2010 Elsevier B.V. All rights reserved.
doi:10.1016/j.jconrel.2010.02.002

various types of tumors and are usually associated with tumor progression and poor prognosis (reviewed in [25]). Inhibition of VEGF or its signaling pathway has been shown to suppress tumor angiogenesis and tumor growth [reviewed in [25–27]].

The soluble form of VEGF receptor-1 (soluble fms-like tyrosine kinase-1: sFlt-1) is a potent endogenous agent for antiangiogenic therapy. The sFlt-1 binds to VEGF with the same affinity and equivalent specificity as that of the original receptor, however inhibits its signal transduction [28–30]. Therefore, exogenous sFlt-1 is considered to be an effective therapeutic agent for antiangiogenic tumor therapy [20,21,31–35]. Recently, several reports were published on *in vivo* non-viral gene therapy with sFlt-1, carried by several types of polymers, for inhibition of tumor angiogenesis [21,35]. Kim WJ et al. reported effective tumor growth suppression in CT-26 colon adenocarcinoma bearing mice by systemic injection of polyethyleneimine based polyplexes, utilizing the RGD targeting approach [21].

In this study, thiolated PEG-poly(L-lysine) (PEG-PLys) block copolymer, combining long PEG chain with optimized crosslinking degree, was designed for construction of RGD-mediated gene delivery system. Here we report the therapeutic effect of sFlt-1 expressing pDNA complexed with 15% thiolated control poly(ethylene glycol)-*block*-poly(L-lysine) (PEG-P(Lys-SH15)) and cyclic RGD conjugated (c(RGDfK)-PEG-P(Lys-SH15)) polymers, forming crosslinked polyplex micelles, after systemic administration to BxPC3 human pancreas adenocarcinoma tumor bearing mice. Note that BxPC3 xenografts are characterized by heterogeneous vascularity and stroma-rich histology [36], which limits access of therapeutic agents to tumor cells. Thus, the accessibility of endothelial cells by bloodstream, makes antiangiogenic approach an attractive strategy against pancreatic tumor.

2. Materials and methods

2.1. Materials

N-Succinimidyl 3-(2-pyridyldithio)-propionate (SPDP) was purchased from Dojindo Laboratories (Kumamoto, Japan). Cyclo[RGDfK(CX-)] (c(RGDfK)) peptides (X = 6-aminocaproic acid: ε-Acp) was purchased from Peptide Institute (Osaka, Japan). The PEG-PLys block copolymer (PEG, 17,000 g/mol; polymerization degree of PLys segment, 73) was synthesized as previously reported [37]. Plasmid DNA coding for luciferase (Luc) under the control of CAG promoter was provided by RIKEN Gene Bank (Tsukuba, Japan), and a fragment cDNA of sFlt-1 was inserted into the pCAcc vector having CAG promoter. The pDNAs were amplified in competent DH5α *Escherichia coli* and purified by the HiSpeed Plasmid Maxi Kit purchased from QIAGEN Sciences Co., Inc. (Germantown, MD). Luc pDNA was labeled with Cy5 by the Label IT Nucleic Acid Labeling Kit (Mirus, Madison, WI) according to the manufacturer's protocol. Dulbecco's modified eagle's medium (DMEM) and fetal bovine serum (FBS) were obtained from Sigma-Aldrich Co (Madison, WI) and Dainippon Sumimoto Pharma Co., Ltd. (Osaka, Japan), respectively. Rat monoclonal antibody to CD31 (platelet endothelial cell adhesion molecule 1 (PECAM1)) was purchased from BD Pharmingen (Franklin Lakes, NJ), and Alexa Fluor 488-conjugated secondary antibody to rat IgG was from Invitrogen Molecular Probes (Eugene, OR).

2.2. Preparation of block copolymers

2.2.1. Synthesis of thiolated PEG-PLys (PEG-P(Lys-SH))

Pyridyldithiopropionyl (PDP) groups were introduced to the ε-amino groups of PLys side chain as reported previously [12]. Briefly, acetal-PEG-PLys (83 mg, 2.86 μmol) was dissolved in 10 mL *N*-methyl-2-pyrrolidone containing 5 wt.% LiCl and stirred with a heterobifunctional reagent, SPDP, (10 mg, 31 μmol) in the presence of *N*,*N*-diisopropylethylamine (10 mol excess against the SPDP reagent) for 3 h at room temperature. The mixture was then precipitated into 20 times excess volume of diethyl ether. The precipitated polymer was dissolved in 10 mM phosphate buffer (pH 7.0, 150 mM NaCl), dialyzed against the same buffer and then distilled water, and lyophilized to obtain PEG-P(Lys-PDP). The degree of PDP substitution for each polymer was determined from the peak intensity ratio of the methylene protons of PEG (OCH_2CH_2, $\delta = 3.5$ ppm) to the pyridyl protons of the 3-(2-pyridyldithio)propionyl group (C_5H_4N, $\delta = 7.2$–8.3 ppm) in the ^{1}H NMR spectrum (D_2O, 25 °C). Block copolymer with X % thiolation degree was abbreviated as B-SHX%.

2.2.2. Synthesis of c(RGDfK)-PEG-P(Lys-SH)

Acetal-PEG-P(Lys-PDP) (30 mg, 1 μmol) was dissolved in 10 mM Tris–HCl buffer solution (pH 7.4) (3 mL) with 10 eq. of dithiothreitol (DTT). After 30 min incubation at room temperature, the polymer solution was dialyzed against 0.2 M AcOH buffer (pH 4.0). c[RGDfK(CX-)] (8 mg, 6.5 mmol) in AcOH buffer (3 mL) was then added to the polymer solution. After stirring for 5 days, DTT (6.67 mg, 43.9 μmol) was added and stirred at room temperature for 3 h. The reacted polymer was purified by dialysis sequentially against 10 mM phosphate buffer pH 7.0 with 150 mM NaCl and distilled water, and lyophilized to obtain c(RGDfK)-PEG-P(Lys-SH) [14].

2.3. Preparation of polyplex micelles

The above polymers were dissolved in 10 mM Tris–HCl buffer (pH 7.4) containing 10% volume of 100 mM DTT. After 30 min at ambient temperature, twice-excess volume of pDNA solution (50 μg/mL) in the same buffer was added to the polymer solution to form a polyplex micelle at *N/P* ratio of 2. The *N/P* ratio was defined as the residual molar ratio of amino groups of thiolated PEG-PLys to phosphate groups of pDNA. After an overnight incubation at ambient temperature, the polyplex micelle solutions were dialyzed against 10 mM Tris–HCl (pH 7.4) containing 0.5% dimethylsulfoxide (DMSO) at 37 °C for 24 h, followed by additional 2 days dialysis for the DMSO removal. During these dialysis processes, thiol groups of the polymers in the micelles were oxidized to form disulfide crosslinks. The concentration of pDNA in each micelle solution was determined by absorbance at 260 nm. Polyplex micelles with and without cyclic RGD peptide ligands were abbreviated as RGD(+) and RGD(−), respectively.

2.4. Quantitative determination of transfection efficiency by real time reverse transcription-polymerase chain reaction (RT-PCR) for sFlt-1

HeLa cells, expressing the $\alpha_v\beta_3$ and $\alpha_v\beta_5$ integrin receptors, were seeded on 24-well culture plates (10000 cells/well) and incubated for 24 h in 500 μL of DMEM medium containing 10% FBS. Micelle solutions were then added at a concentration equivalent to 1 μg of pDNA per well and the cells were incubated for 48 h. Following this incubation period, total RNA was extracted from the cells and transcripted to cDNA. The cDNA samples were subjected to polymerase chain reaction (PCR) amplification using the following human specific primers: 5′-CCACTCCCTTGAACACGAG-3′ and 3′-CGCCTTACG-GAAGCTCTCT-5′. Amplification conditions were as recommended by the manufacturer (QIAGEN Sciences Co., Inc.). Unknown and standard samples were run in triplicate. Concentrations of unknown samples were interpolated from a standard curve, established by simultaneous amplification of sFlt-1 plasmid standards.

2.5. In vivo studies

2.5.1. Mice

Five-week-old female Balb/c nude mice were purchased from Charles River Laboratories (Tokyo, Japan). Mice were maintained on ad libitum rodent feed and water. The experimental animals were allowed to acclimate for at least 1 week before tumor implantation. All studies were performed in accordance to the Guide for the Care

and Use of Laboratory Animals as stated by the National Institutes of Health.

2.5.2. Tumor implantation

BxPC3 cell line (ATCC, Manassas, VA), derived from human pancreatic tumor was inoculated to nude mice subcutaneously to develop xenografts (100 μl of 5×10^7 cells/mL PBS suspension). Tumors were allowed to grow for 3 weeks till their size reached approximately 120–160 mm^3.

2.5.3. Blood circulation

Polyplex micelles loading Cy5-labeled pDNA (100 μg pDNA/mL, 200 μL) were intravenously injected to the mice via the tail vein at a dose of 20 μg pDNA/mouse. Blood was collected from the postcaval vein under anesthesia 15 min after injection and centrifuged to obtain blood plasma. Two microliters of 10X trypsin-EDTA were added to 20 μL of the plasma and incubated overnight at 37 °C to release pDNA from the micelle by digesting PLys segment of the block copolymer. The fluorescence intensity of the sample solution was measured at $\lambda = 670$ nm by spectrofluorometer (ND-3300, Nano Drop, Wilmington, DE), and percent of pDNA dosage in the blood was calculated according to the following equation:

$$\%\ \text{injected pDNA in the blood} = (F_{670(\text{sample})} / F_{670(\text{control})}) \times 100 \quad (1)$$

where the $F_{670(\text{control})}$ represents the fluorescence intensity of micelle solution mixed with blood sample (time 0).

2.5.4. In vivo tumor growth inhibition

Polyplex micelles, loading pDNA equivalent to 20 μg and dissolved in 10 mM Hepes buffer (pH 7.4) with 150 mM NaCl, were administered intravenously on days 0, 4, and 8. Tumor size was measured every 2 days by a digital vernier caliper across its longest (a) and shortest diameters (b) and its volume (V) was calculated according to the formula $V = 0.5ab^2$. Tumor progression was evaluated in terms of relative tumor volume (to day 0) over a period of 18 days.

2.5.5. Quantification of microvessel density

At the end of *in vivo* tumor growth studies, xenografted tumors were excised and frozen in tissue-Tek-OCT. The frozen tumors were cut into 10 μm thick slices with a cryostat maintained at −23 °C. Vascular endothelial cells were immunostained by incubation of the cryosections with anti-CD31 antibody followed by incubation with Alexa Fluor 488-conjugated secondary antibody. The tumor cryosections were observed by a confocal laser scanning microscope (CLSM), LSM 510 (Carl Zeiss, Oberlochen, Germany). Microvessel density was quantified by counting the percentage area of CD31 positive pixels per image with at least 21 images per sample (i.e., three animals per sample x 7 cryosections per tumor).

2.5.6. Micelle accumulation in tumor tissue

Polyplex micelles loading Cy5-labeled pDNA were intravenously injected at a dose of 20 μg pDNA/mouse. Mice were sacrificed after 24 h and the excised tumors were fixed in formalin for 1 h, followed by 1 h incubation periods with 10, 15 and 20% sucrose/PBS solutions at room temperature. The tumors were frozen in tissue-Tek-OCT and cryosections were prepared for CLSM visualizations as described in the previous section. The nuclei were stained with Hoechst 33342 (Dojindo Lab., Kumamoto, Japan). The CLSM observations were performed at the excitation wavelengths of 488 nm (Ar laser) for the Alexa Fluor 488, 633 nm (He–Ne laser) for Cy5, and 710 nm (MaiTai laser, two photon excitation) for Hoechst 33342, respectively. The percentage of pDNA positive pixels per image was counted to quantify the micelle accumulation inside the tumor tissue.

2.6. Data analysis

The experimental data was analyzed by Student's *t*-test. $P < 0.05$ was considered as significant.

3. Results

Thiolated acetal-PEG-PLys block copolymers, composed of 17 kDa M.W. PEG and 73 lysine units, were prepared as described elsewhere [12,14,37]. SPDP was used as a thiolating reagent and conjugated to the ε-amino group of lysine unit. Conjugation of c(RGDfK) peptide ligands into the PEG terminus of acetal-PEG-P(Lys-PDP) was achieved through the formation of a thiazolidine ring between the *N*-terminal cysteine and the aldehyde group converted from the acetal group [14,15]. The targetable polyplex micelles were prepared through ion complexation of the above polymers with pDNA at $N/P = 2$ (Fig. 1), and analyzed for their size and ζ-potential by DLS and laser-doppler electrophorsis, respectively. The cumulant diameters of the B-SHX% micelles were approximately 104 ± 18 nm, with a moderate polydispersity index of 0.2. The ζ-potentials were found to be approximately 0.5 mV, as a result of the PEG palisade formation surrounding the polyplex core [8,14].

Following *in vitro* transfection in HeLa cells, the mRNA expressions of sFlt-1 were quantitatively analyzed by real time RT-PCR. From this analysis, presented in Fig. 2, it is clear that the cells were successfully transfected by the polyplex micelles. The highest transfection efficiency was achieved by RGD(+) B-SH15% crosslinked (15(+)) micelle. Worth noting, detectable protein level of sFlt-1 by ELISA, specific to human VEGF-R1/sFlt-1 (R&D Systems), could be achieved for this formulation only (1.2 ± 0.05 ng/mL) (data not shown). Other micelles, probably, resulted in sFlt-1 levels which are beyond the sensitivity of this assay (<13 pg/ml). The increased transfection efficiency of the 15(+) micelle results from the combination of crosslinked core and receptor targeting ligand, consistent with our previous studies [15].

The blood circulation experiments were carried out in BxPC3 tumor bearing mice upon intravenous injections of the Cy5-labeled pDNA (20 μg pDNA/ mouse). Blood was collected from the postcaval vein 15 min after administration and analyzed for its fluorescence intensity. Disulfide crosslinks prolonged blood circulation time, while the RGD conjugation resulted in significantly lower blood circulation period of polyplex micelles, as shown in Fig. 3. In the case of crosslinked system, 28% and 21% of injected pDNA were observed in plasma for RGD(−) and RGD(+) micelles, respectively. Significantly lower recovered doses of pDNA, 11 % and 7 % for RGD(−) and RGD(−) micelles, respectively, were found for non crosslinked system. We further evaluated micelle accumulation in tumor by iv administration of RGD-conjugated or non-conjugated 15% crosslinked micelles prepared with Cy5-labeled pDNA at a dose of 20 μg pDNA/mouse. Both micelles were found to be localized in the tumor blood vessels, 24 h after administration, as was indicated by colocalization of the Cy5-labeled pDNA (red) and the CD31 positive endothelial cells (green) (Fig. 4A). However, quantitative analysis of the pDNA positive area per image revealed significantly higher accumulation of the RGD-conjugated micelle than non-conjugated micelle inside the tumor tissue (Fig. 4B): 3.08 % and 2.44 % of red pixels per image for RGD(−) and RGD(−) micelle, respectively ($P < 0.05$).

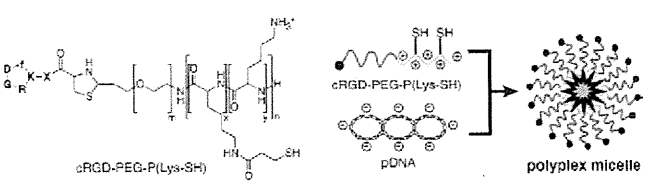

Fig. 1. Structure of cRGD-PEG-P(Lys-SH) and its polyplex micelle.

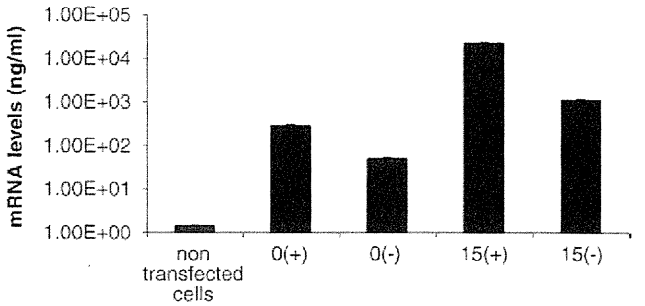

Fig. 2. *In vitro* transfection efficiency of sFlt-1 plasmid DNA in HeLa cells. The cells were transfected with RGD(+) and RGD(−) non crosslinked micelles (0(−) and 0(−)) and RGD(+) and RGD(−) 15% crosslinked micelles (15(−) and 15(−)), respectively. Non transfected cells were used as control. Each well was transfected with 1 μg of pDNA for 48 h and analyzed for sFlt-1 mRNA levels by real time RT-PCR.

The therapeutic effect of polyplex micelles following intravenous administration of the sFlt-1 expressing pDNA was evaluated by tumor growth inhibition study in BxPC3 tumor bearing mice. When tumors reached the volume of 120–160 mm^3, animals were injected with three doses of polyplex micelles containing either sFlt-1 or Luc expressing plasmid (20 μg pDNA/dose) on days 0, 4 and 8. The results of these studies, in terms of relative tumor volumes (Fig. 5), indicate the ability of RGD(+) and RGD(−) crosslinked polyplex micelles as vehicles for therapeutic gene delivery in BxPC3 tumor bearing mice. In the case of animals treated with 15(−) micelles, the tumor progression was significantly inhibited from day 6, compared to control mice. By the end of the experiment, the mean tumor volume in this group was 1.67 ± 0.18 of initial tumor volume. In the group of animals treated with pDNA encapsulated in RGD(−) micelles, significant inhibition of tumor progression was observed only from day 12, and the mean tumor volume reached 1.93 ± 0.52 of initial tumor volume by the end of the experiment. On the other hand, tumors grew much faster in the control groups, and reached 2.58 ± 0.5 of initial tumor volume.

Intravenous administration of crosslinked polyplex micelles containing sFlt-1 pDNA to BxPC3 tumor bearing mice resulted in significant reduction in the tumor neo-vasculature, as shown by CD31 immunostaining of the tumor cryosections. Representative images are shown in Fig. 6A. Increased density of blood vessels throughout the tissue was observed in control tumors. In contrast, very few blood vessels could be observed in the sFlt-1 treated groups. The quantitative results of microvessel density in tumor tissue cryosections were obtained by counting the area of stained blood vessels (green pixels) per image (Fig. 6B). Systemic administration of sFlt-1 expressing pDNA in the RGD(+) micelles resulted in the lowest average microvessel density of only 8.6% per image, whereas the RGD (−) micelle carrying pDNA led to 12.3% vessels per image. The control group had an average microvessel area of 23.7% per image, significantly higher as compared to the treated groups.

4. Discussion

In this study, we demonstrate that crosslinked polyplex micelles formed by electrostatic interaction of thiolated PEG-PLys block copolymers, modified on their surface with cRGD peptide ligand, and sFlt-1 pDNA are effective for *in vivo* tumor regression upon systemic administration. The thiolated PEG-PLys block copolymer, in this study, was further optimized by higher molecular weight PEG (17,000 Da) against 12,000 Da M.W. PEG used so far [2,3,8,12–15], to achieve enhanced shielding effect and thus higher stability in blood. Block copolymer with 15% thiolation degree, which showed the highest transfection efficiency *in vitro* and *in vivo* (data not shown), was selected for construction of RGD-mediated gene delivery vector.

The results of sFlt-1 transfection in Hela cells show higher mRNA expression levels in the cells transfected by RGD(−) crosslinked micelle relative to either RGD(−) or non crosslinked micelles (Fig. 2). This result is consistent with our previous studies, indicating the greater stability of crosslinked micelles in the medium and specific affinity of RGD ligand to $\alpha_v\beta_3$ and $\alpha_v\beta_5$ integrin receptors expressed in HeLa cells [14,15]. Micelle internalization to the cell via integrin-mediated endocytosis contributes to the accelerated accumulation of pDNA in the perinuclear region through the change in its intracellular trafficking from clathrin-mediated to caveolae-mediated endocytosis, resulting in enhancement of gene expression [15].

When administrated intravenously into BxPC3 tumor bearing mice, blood levels of Cy5-labeled pDNA were significantly lower for the RGD(+) micelle compared to the RGD(−) micelle. This observation might be partly explained by enhanced accumulation of pDNA in tumor site when carried by RGD(−) micelle over RGD(−) (Fig. 4B) and other organs as well. These observations are in good agreement with other works using cyclic RGD-modified particles, which reported significantly lower blood circulation times [38–40] while higher accumulation in tumor tissue [21,38–41], liver [21,38–42] and spleen [28–31] compared to the control. Moreover, CLSM observations demonstrated colocalization of both micelles with tumor endothelial cells, confirming their potential as effective antiangiogenic gene delivery vehicles (Fig. 4A).

In vivo tumor growth assay revealed significant ($P<0.05$) tumor growth inhibition when the sFlt-1 pDNA was administrated by crosslinked micelles as compared to control groups. Compared to RGD(−), the RGD(+) micelle was more effective in suppressing tumor growth. The significant difference in relative tumor volumes between RGD(−) injected and control groups was observed from day 6 till the end of the experiment. In comparison, significant difference between RGD(−) injected and control groups was observed only from day 12. In addition, relative tumor volumes in the RGD(−) injected group were lower than those in the RGD(−). These findings may be explained by greater tumor accumulation and higher transfection efficiency of RGD-modified micelle, resulted from more effective intracellular plasmid delivery through specific receptor binding and endocytosis. The lack of significant difference in relative tumor volumes between the RGD(−) and RGD(−) injected groups might be due to the lower circulation time in blood of the RGD(−) micelle and its enhanced accumulation in organs such as liver and spleen. Accumulation in liver [21,38–42] and spleen [39–42] was shown for various cyclic RGD-modified vectors and was, in general, attributed to their accelerated clearance through the phagocytosis by macrophages located on reticuloendothelial system (RES) [39–41].

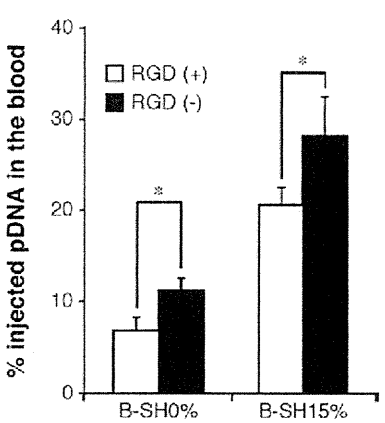

Fig. 3. Blood circulation of plasmid DNA carried by RGD (+/−) polyplex micelles. Micelles loading Cy5-labeled pDNA were intravenously administrated to the tumor bearing mice (20 μg pDNA/mouse). Blood was collected 15 min after administration and analyzed for its fluorescence intensity. $N=3$, Mean ± s.d. *$P<0.05$ compared to RGD(−).

The antiangiogenic effect of expressed sFlt-1 was confirmed by CD31 immunostaining of the tumor cryosections and quantification of microvessel density. From these studies, it is clear that sFlt-1 was able to significantly suppress tumor neo-vasculature formation when the pDNA was delivered in RGD(+) and RGD(−) crosslinked micelles. The most pronounced effect on microvessel density was observed with the plasmid administrated in RGD(+) micelles. This is probably due to the combined effect of tumor accumulation and increased transfection efficiency of the RGD-conjugated 15% crosslinked polyplex micelle.

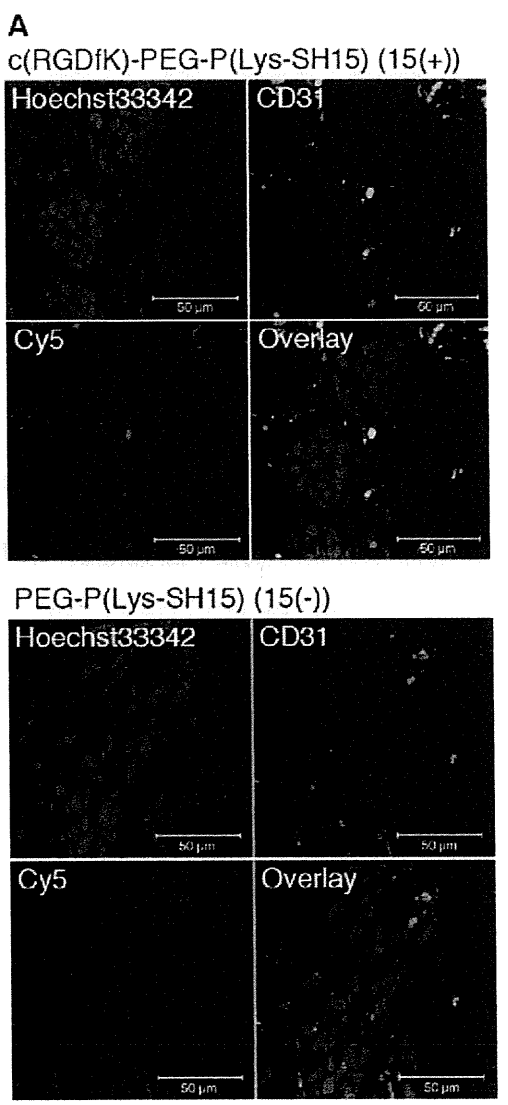

Fig. 4. Micelle localization in tumor tissue. (A) Tumor endothelium and pDNA localization. Immunostaining of CD31 (green) revealed colocalization of Cy5-labeled pDNA (red) with tumor vasculature for both RGD-conjugated (15(−)) and non-conjugated (15(−)) micelles, 24 h after administration. The cell nuclei were stained with Hoechst 33342 (blue). (B) Quantitative analysis of Cy5-labeled pDNA (red pixels). The results represent percentage areas of pDNA-positive pixels per image. Seven images were taken from each tumor tissue, from 3 mice, mean ± s.d.

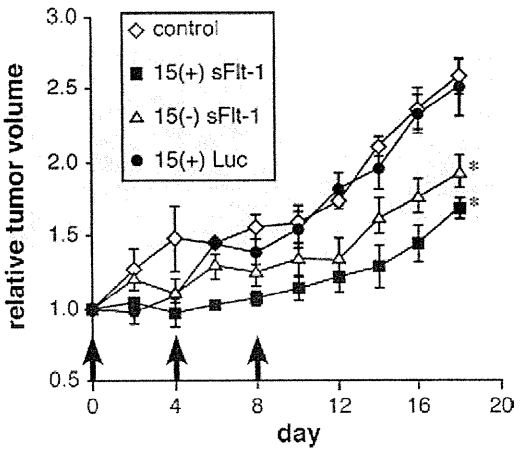

Fig. 5. *In vivo* tumor growth inhibition. RGD (−) and RGD (−) 15% crosslinked polyplex micelles loading plasmid DNA coding either sFlt-1 or Luc were administrated intravenously to BxPC3 tumor bearing mice at a pDNA dose of 20 μg on days 0, 4 and 8, as indicated by arrows. Control animals were injected with either Hepes buffer or 15 (−) micelle loading Luc expressing pDNA. Tumor volumes were measured every 2 days up to day 18 and normalized to the initial tumor volume (day 0). Results are presented in terms of relative tumor volumes, mean ± s.d., $N = 6$. $^*P < 0.05$ compared to control group.

5. Conclusion

Our data contributes to the list of successful non-viral systems for antiangiogenic cancer gene therapy utilizing sFlt-1 pDNA as VEGF sequester [21,35] and RGD targeting of tumor endothelial cells [19,21]. Worth noting, the antiangiogenic gene therapy by sFlt-1 pDNA, delivered by non-viral vector with cRGD ligand, appears to be a promising strategy to treat an intractable pancreatic tumor.

The significant inhibitory effect of tumor growth shown in this study, confirms the potential of c(RGDfK)-PEG-P(Lys-SH15) and PEG-P(Lys-SH15) polyplex micelles as effective systemic gene delivery systems to the neo-vasculature of solid tumors. Both of these formulations showed accumulation and interaction with tumor endothelial cells. The therapeutic activity of c(RGDfK)-PEG-P(Lys-SH15) was pronounced by combined effect of increased tumor accumulation and enhanced intracellular delivery. Based on these studies, c(RGDfK)-PEG-P(Lys-SH15) can be employed as an effective platform for systemic administration of therapeutic plasmid DNA for antiangiogenic therapy.

Acknowledgement

This work was financially supported in part by the Core Research Program for Evolutional Science and Technology (CREST) from Japan

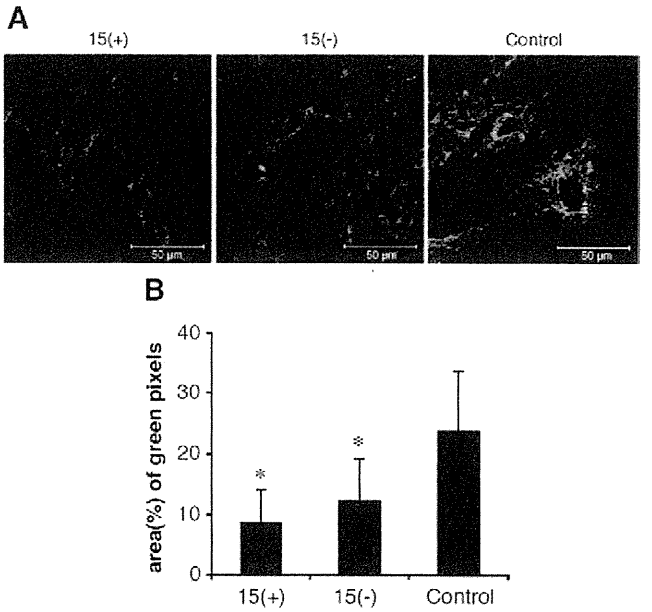

Fig. 6. Antiangiogenic effect of expressed sFlt-1 in BxPC3 tumor bearing mice. Tumor microvessels were detected by CD31 (PECAM1) antibody staining of tumor cryosections 20 days after therapy. (A) Representative CD31 immunostaining images. (B) Quantitative analysis of microvessel density in tumor cryosections. The results represent a percentage area of green pixels per image. Seven images were taken from each tumor tissue, from 3 mice, mean ± s.d. $^{*}P<0.05$ compared to control group.

Science and Technology Agency (JST) as well as by Grants-in-Aid for Young Scientists (A). We express our appreciation to Prof. M. Shibuya (Tokyo Medical and Dental University) for providing pVL 1393 baculovirus vector pDNA encoding human sFlt-1. We thank Ms. S. Ogura (The University of Tokyo) for her technical assistance.

References

[1] A. Harada, K. Kataoka, Formation of polycation complex micelles in an aqueous milieu from a pair of oppositely-charged block copolymers with poly(ethylene glycol) segments, Macromolecules 28 (15) (1995) 5294–5299.
[2] S. Katayose, K. Kataoka, Water-soluble polyion complex associates of DNA and poly(ethylene glycol)-poly(L-lysine) block copolymer, Bioconjug. Chem. 8 (5) (1997) 702–707.
[3] M. Harada-Shiba, K. Yamauchi, A. Harada, I. Takamisawa, K. Shimokado, K. Kataoka, Polyion complex micelles as vectors in gene therapy – pharmacokinetics and in vivo gene transfer, Gene Ther. 9 (6) (2002) 407–414.
[4] M. Laus, K. Sparnacci, B. Ensoli, S.O. Buttò, A. Caputo, I. Mantovani, G. Zuccheri, B. Samorì, L. Tondelli, Complex associates of plasmid DNA and a novel class of block copolymers with PEG and cationic segments as new vectors for gene delivery, J. Biomater. Sci. Polym. Ed. 12 (2) (2001) 209–228.
[5] C.H. Ahn, S.Y. Chae, Y.H. Bae, S.W. Kim, Synthesis of biodegradable multi-block copolymers of poly(L-lysine) and poly(ethylene glycol) as a non-viral gene carrier, J. Control. Release 97 (3) (2004) 567–574.
[6] Y. Wang, C.Y. Ke, B.C. Weijie, S.Q. Liu, S.H. Goh, Y.Y. Yang, The self-assembly of biodegradable cationic polymer micelles as vectors for gene transfection, Biomaterials 28 (35) (2007) 5358–5368.
[7] Y.R. Choi, S.Y. Chae, C.H. Ahn, M. Lee, S. Oh, Y. Byun, B.D. Rhee, K.S. Ko, Development of polymeric gene delivery carriers: PEGylated copolymers of L-lysine and L-phenylalanine, J. Drug Target. 15 (6) (2007) 391–398.
[8] K. Itaka, K. Yamauchi, A. Harada, K. Nakamura, H. Kawaguchi, K. Kataoka, Polyion complex micelles from plasmid DNA and poly(ethylene glycol)-poly(L-lysine) block copolymer as serum-tolerable polyplex system: physicochemical properties of micelles relevant to gene transfection efficiency, Biomaterials 24 (24) (2003) 4495–4506.
[9] S. Mishra, P. Webster, M.E. Davis, PEGylation significantly affects cellular uptake and intracellular trafficking of non-viral gene delivery particles, Eur. J. Cell Biol. 83 (3) (2004) 97–111.
[10] A.M. Funhoff, S. Monge, R. Teeuwen, G.A. Koning, N.M. Schuurmans-Nieuwenbroek, D.J. Crommelin, D.M. Haddleton, W.E. Hennink, C.F. van Nostrum, PEG shielded polymeric double-layered micelles for gene delivery, J. Control. Release 102 (3) (2005) 711–724.
[11] H.K. de Wolf, C.J. Snel, F.J. Verbaan, R.M. Schiffelers, W.E. Hennink, G. Storm, Effect of cationic carriers on the pharmacokinetics and tumor localization of nucleic acids after intravenous administration, Int. J. Pharm. 331 (2) (2007) 167–175.
[12] K. Miyata, Y. Kakizawa, N. Nishiyama, A. Harada, Y. Yamasaki, H. Koyama, K. Kataoka, Block catiomer polyplexes with regulated densities of charge and disulfide cross-linking directed to enhance gene expression, J. Am. Chem. Soc. 126 (8) (2004) 2355–2361.
[13] K. Miyata, Y. Kakizawa, N. Nishiyama, Y. Yamasaki, T. Watanabe, M. Kohara, K. Kataoka, Freeze-dried formulations for in vivo gene delivery of PEGylated polyplex micelles with disulfide crosslinked cores to the liver, J. Control. Release 109 (1–3) (2005) 15–23.
[14] M. Oba, S. Fukushima, N. Kanayama, K. Aoyagi, N. Nishiyama, H. Koyama, K. Kataoka, Cyclic RGD peptide-conjugated polyplex micelles as a targetable gene delivery system directed to cells possessing $\alpha_v\beta_3$ and $\alpha_v\beta_5$ integrins, Bioconjug. Chem. 18 (5) (2007) 1415–1423.
[15] M. Oba, K. Aoyagi, K. Miyata, Y. Matsumoto, K. Itaka, N. Nishiyama, Y. Yamasaki, H. Koyama, K. Kataoka, Polyplex Micelles with cyclic RGD peptide ligands and disulfide cross-links directing to the enhanced transfection via controlled intracellular trafficking, Mol. Pharmaceutics 5 (6) (2008) 1080–1092.
[16] M.D. Pierschbacher, E. Ruoslahti, Cell attachment activity of fibronectin can be duplicated by small synthetic fragments of the molecule, Nature 309 (5963) (1984) 30–33.
[17] R. Haubner, R. Gratias, B. Diefenbach, S.L. Goodman, A. Jonczyk, H. Kessler, Structural and functional aspects of RGD-containing cyclic pentapeptides as highly potent and selective integrin $\alpha_v\beta_3$ antagonists, J. Am. Chem. Soc. 118 (1996) 7461–7472.
[18] A. Erdreich-Epstein, H. Shimada, S. Groshen, M. Liu, L.S. Metelitsa, K.S. Kim, M.F. Stins, R.C. Seeger, D.L. Durden, Integrins alpha(v)beta3 and alpha(v)beta5 are expressed by endothelium of high-risk neuroblastoma and their inhibition is associated with increased endogenous ceramide, Cancer Res. 60 (3) (2000) 712–721.
[19] R.M. Schiffelers, A. Ansari, J. Xu, Q. Zhou, Q. Tang, G. Storm, G. Molema, P.Y. Lu, P.V. Scaria, M.C. Woodle, Cancer siRNA therapy by tumor selective delivery with ligand-targeted sterically stabilized nanoparticle, Nucleic Acids Res. 32 (19) (2004) e149.
[20] W.J. Kim, J.W. Yockman, M. Lee, J.H. Jeong, Y.H. Kim, S.W. Kim, Soluble Flt-1 gene delivery using PEI-g-PEG-RGD conjugate for anti-angiogenesis, J. Control. Release 106 (1–2) (2005) 224–234.
[21] W.J. Kim, J.W. Yockman, J.H. Jeong, L.V. Christensen, M. Lee, Y.H. Kim, S.W. Kim, Anti-angiogenic inhibition of tumor growth by systemic delivery of PEI-g-PEG-RGD/pCMV-sFlt-1 complexes in tumor-bearing mice, J. Control. Release 114 (3) (2006) 381–388.
[22] K. Temming, R.M. Schiffelers, G. Molema, R.J. Kok, RGD-based strategies for selective delivery of therapeutics and imaging agents to the tumor vasculature, Drug Resist. Updat. 8 (6) (2005) 381–402.
[23] K.A. Thomas, Vascular endothelial growth factor, a potent and selective angiogenic agent, J. Biol. Chem. 271 (2) (1996) 603–606.
[24] G. Breier, Functions of the VEGF/VEGF receptor system in the vascular system, Semin. Thromb. Hemost. 26 (5) (2000) 553–559.
[25] R.A. Brekken, P.E. Thorpe, VEGF-VEGF receptor complexes as markers of tumor vascular endothelium, J. Control. Release 74 (1–3) (2001) 173–181.
[26] A.L. Harris, Anti-angiogenesis therapy and strategies for integrating it with adjuvant therapy, Recent Results Cancer Res. 152 (1998) 341–352.
[27] N. Ferrara, VEGF as a therapeutic target in cancer, Oncology 69 (2005) 11–16.
[28] R.L. Kendall, G. Wang, K.A. Thomas, Identification of a natural soluble form of the vascular endothelial growth factor receptor, FLT-1, and its heterodimerization with KDR, Biochem. Biophys. Res. Commun. 226 (2) (1996) 324–328.
[29] H. Chen, U. Ikeda, M. Shimpo, Y. Maeda, M. Shibuya, K. Ozawa, K. Shimada, Inhibition of vascular endothelial growth factor activity by transfection with the soluble FLT-1 gene, J. Cardiovasc. Pharmacol. 36 (4) (2000) 498–502.
[30] M. Malecki, H. Trembacz, B. Szaniawska, M. Przybyszewska, P. Janik, Vascular endothelial growth factor and soluble FLT-1 receptor interactions and biological implications, Oncol. Rep. 14 (6) (2005) 1565–1569.
[31] C. Ye, C. Feng, S. Wang, K.Z. Wang, N. Huang, X. Liu, Y. Lin, M. Li, sFlt-1 gene therapy of follicular thyroid carcinoma, Endocrinology 145 (2) (2004) 817–822.
[32] Y. Hasumi, H. Mizukami, M. Urabe, T. Kohno, K. Takeuchi, A. Kume, M. Momoeda, H. Yoshikawa, T. Tsuruo, M. Shibuya, Y. Taketani, K. Ozawa, Soluble FLT-1 expression suppresses carcinomatous ascites in nude mice bearing ovarian cancer, Cancer Res. 62 (7) (2002) 2019–2023.
[33] G. Mahendra, S. Kumar, T. Isayeva, P.J. Mahasreshti, D.T. Curiel, C.R. Stockardt, W.E. Grizzle, V. Alapati, R. Singh, G.P. Siegal, S. Meleth, S. Ponnazhagan, Antiangiogenic cancer gene therapy by adeno-associated virus 2-mediated stable expression of the soluble FMS-like tyrosine kinase-1 receptor, Cancer Gene Ther. 12 (1) (2005) 26–34.
[34] Y. Takei, H. Mizukami, Y. Saga, I. Yoshimura, Y. Hasumi, T. Takayama, T. Kohno, T. Matsushita, T. Okada, A. Kume, M. Suzuki, K. Ozawa, Suppression of ovarian cancer by muscle-mediated expression of soluble VEGFR-1/Flt-1 using adeno-associated virus serotype 1-derived vector, Int. J. Cancer 120 (2) (2007) 278–284.
[35] S. Kommareddy, M. Amiji, Antiangiogenic gene therapy with systemically administered sFlt-1 plasmid DNA in engineered gelatin-based nanovectors, Cancer Gene Ther. 14 (5) (2007) 488–498.
[36] M.R. Kano, Y. Komuta, C. Iwata, M. Oka, Y.T. Shirai, Y. Morishita, Y. Ouchi, K. Kataoka, K. Miyazono, Comparison of the effects of the kinase inhibitors imatinib, sorafenib, and transforming growth factor-beta receptor inhibitor on extravasation of nanoparticles from neovasculature, Cancer Sci. 100 (1) (2009) 173–180.
[37] A. Harada, K. Kataoka, Formation of polyion complex micelles in an aqueous milieu from a pair of oppositely charged block copolymers with poly(ethylene glycol) segments, Macromolecules 28 (1995) 294–299.

[38] P.K. Dubey, V. Mishra, S. Jain, S. Mahor, S.P. Vyas, Liposomes modified with cyclic RGD peptide for tumor targeting, J. Drug Target. 12 (5) (2004) 257–264.
[39] A.J. Schraa, R.J. Kok, H.E. Moorlag, E.J. Bos, J.H. Proost, D.K. Meijer, L.F. de Leij, G. Molema, Targeting of RGD-modified proteins to tumor vasculature: a pharmacokinetic and cellular distribution study, Int. J. Cancer 102 (5) (2002) 469–475.
[40] R.M. Schiffelers, G.A. Koning, T.L. ten Hagen, M.H. Fens, A.J. Schraa, A.P. Janssen, R.J. Kok, G. Molema, G. Storm, Anti-tumor efficacy of tumor vasculature-targeted liposomal doxorubicin, J. Control. Release 91 (1–2) (2003) 115–122.
[41] A. Mitra, J. Mulholland, A. Nan, E. McNeill, H. Ghandehari, B.R. Line, Targeting tumor angiogenic vasculature using polymer-RGD conjugates, J. Control. Release 102 (1) (2005) 191–201.
[42] D.C. Bibby, J.E. Talmadge, M.K. Dalal, S.G. Kurz, K.M. Chytil, S.E. Barry, D.G. Shand, M. Steiert, Pharmacokinetics and biodistribution of RGD-targeted doxorubicin-loaded nanoparticles in tumor-bearing mice, Int. J. Pharm. 293 (1–2) (2005) 281–290.

Biomaterials 32 (2011) 652–663

Contents lists available at ScienceDirect

Biomaterials

journal homepage: www.elsevier.com/locate/biomaterials

Polyplex micelles prepared from ω-cholesteryl PEG-polycation block copolymers for systemic gene delivery

Makoto Oba [a], Kanjiro Miyata [b], Kensuke Osada [c], R. James Christie [c], Mai Sanjoh [d], Weidong Li [c], Shigeto Fukushima [c], Takehiko Ishii [d], Mitsunobu R. Kano [b,e], Nobuhiro Nishiyama [b], Hiroyuki Koyama [a], Kazunori Kataoka [b,c,d,*]

[a] Department of Clinical Vascular Regeneration, Graduate School of Medicine, The University of Tokyo, 7-3-1 Hongo, Bunkyo-ku, Tokyo 113-8655, Japan
[b] Center for Disease Biology and Integrative Medicine, Graduate School of Medicine, The University of Tokyo, 7-3-1 Hongo, Bunkyo-ku, Tokyo 113-0033, Japan
[c] Department of Materials Engineering, Graduate School of Engineering, The University of Tokyo, 7-3-1 Hongo, Bunkyo-ku, Tokyo 113-8656, Japan
[d] Department of Bioengineering, Graduate School of Engineering, The University of Tokyo, 7-3-1 Hongo, Bunkyo-ku, Tokyo 113-8656, Japan
[e] Department of Molecular Pathology, Graduate School of Medicine, The University of Tokyo, 7-3-1 Hong, Bunkyo-ku, Tokyo 113-8655, Japan

ARTICLE INFO

Article history:
Received 11 August 2010
Accepted 24 August 2010
Available online 6 October 2010

Keywords:
Non-viral gene vector
Polyplex micelle
Cholesterol
Pancreatic tumor
Anti-angiogenic therapy

ABSTRACT

Polyplex micelles formed with plasmid DNA (pDNA) and poly(ethylene glycol) (PEG)-*block*-poly{*N*-[*N*-(2-aminoethyl)-2-aminoethyl]aspartamide} [PAsp(DET)] exhibit effective endosomal escaping properties based on di-protonation of diamine side chains with decreasing pH, which improves their transfection efficiency and thus are promising candidates for local *in vivo* gene transfer. Here, PEG-PAsp(DET) polyplex micelles were further improved as *in vivo* systemic vectors by introduction of cholesterol (Chole) into the ω-terminus of PEG-PAsp(DET) to obtain PEG-PAsp(DET)-Chole. Introduction of the cholesterol resulted in enhanced association of block copolymers with pDNA, which led to increased stability in proteinous medium and also in the blood stream after systemic injection compared to PEG-PAsp(DET) micelles. The synergistic effect between enhanced polymer association with pDNA and increased micelle stability of PEG-PAsp(DET)-Chole polyplex micelles led to high *in vitro* gene transfer even at relatively low concentrations, due to efficient cellular uptake and effective endosomal escape of block copolymers and pDNA. Finally, PEG-PAsp(DET)-Chole micelles achieved significant suppression of tumor growth following intravenous injection into mice bearing a subcutaneous pancreatic tumor using therapeutic pDNA encoding an anti-angiogenic protein. These results suggest that PEG-PAsp(DET)-Chole micelles can be effective systemic gene vectors for treatment of solid tumors.

1. Introduction

As expectations for gene therapy increase, so have efforts to develop non-viral vectors with high transfection ability and low toxicity [1,2]. Polyplexes, which are composed of polycations and plasmid DNA (pDNA), are expected as alternatives to viral vectors due to the fine-tuned properties for specific applications by altering the structure of the polycation used for polyplex formation [3–5]. Polyplex micelles formed with poly(ethylene glycol) (PEG)-*block*-polycation block copolymers and pDNA are particularly promising candidates [6–8], due to their excellent characteristics as *in vivo* gene vectors [9,10]. The biocompatible PEG shell layer surrounding the polyplex core contributes to high colloidal stability, allows micelles to maintain their initial size of approximately 100 nm, and reduces non-specific interactions with blood components, which are all desirable properties for systemic administration.

Recently, we reported that polyplex micelles prepared with pDNA and PEG-*block*-poly{*N*-[*N*-(2-aminoethyl)-2-aminoethyl] aspartamide} [PEG-PAsp(DET)] [11] achieved successful *in vitro* transfection of primary cells due to effective endosomal escape of pDNA contained in the micelle core. The PAsp(DET), polycationic segment of the block copolymer is characterized by a distinctive two-step protonation behavior in response to pH and possessed endosomal membrane-selective destabilizing capacity upon acidification [12]. Furthermore, PEG-PAsp(DET) polyplex micelles have shown successful *in vivo* gene transfer by local administration in

* Corresponding author. Department of Materials Engineering, Graduate School of Engineering, The University of Tokyo, 7-3-1 Hongo, Bunkyo-ku, Tokyo 113-8656, Japan. Tel.: +81 3 5841 7138; fax: +81 3 5841 7139.
E-mail address: kataoka@bmw.t.u-tokyo.ac.jp (K. Kataoka).

0142-9612/$ – see front matter © 2010 Elsevier Ltd. All rights reserved.
doi:10.1016/j.biomaterials.2010.09.022

several animal models including: a clamped rabbit carotid artery with neointima without vessel occlusion by thrombus [13], a mouse skull by regulated release from a calcium phosphate cement scaffold to induce bone regeneration through the osteogenic factors [14], and a rat lung pulmonary arterial hypertension model via intratracheal administration [15]. In these cases, however, excess block copolymers relative to pDNA (high N/P ratio) were required to achieve high transfection efficiency, suggesting the existence of free polymer. If free polymer plays a significant role for gene transfer with polyplex micelles prepared from PEG-PAsp (DET) and pDNA, the transfection efficiency under highly diluted conditions, such as systemic application, could be drastically decreased.

The aim of this study was to further develop PEG-PAsp(DET) polyplex micelles towards *in vivo* systemic pDNA delivery vectors. In order to enhance the association of PEG-PAsp(DET) polymers with pDNA and thus increase the efficiency of cellular internalization of polymer necessary for improved endosome escaping, we utilized both electrostatic interaction between polycations and pDNA and hydrophobic interaction by cholesterol to form micelles with improved stability. Specifically, cholesterol was introduced onto the ω-terminus of the PAsp(DET) segment in PEG-PAsp(DET) block copolymer. Cholesterol introduction significantly increased the number of block copolymers associating with a pDNA. *In vitro* experiments were done to demonstrate improved transfection efficiency of PEG-PAsp(DET)-Chole polyplex micelles at low N/P ratios and under the diluted conditions compared to the control micelles formed without cholesterol modified block copolymer. Then, the enhanced stability by the cholesterol introduction in blood was shown, thus allowing successful treatment of a subcutaneous tumor by systemic administration of micelles prepared with PEG-PAsp(DET)-Chole and therapeutic pDNA encoding for an anti-angiogenic protein.

2. Materials and methods

2.1. Materials

Dichloromethane (CH_2Cl_2), *N,N*-dimethylformamide (DMF), triethylamine (TEA), and 3-(4,5-dimethylthiazol-2-yl)-2,5-diphenyltetrazolium bromide (MTT) were purchased from Wako Pure Chem. Co. Ltd. (Osaka, Japan). Cholesterol chloroformate was purchased from Aldrich Chemical Co. Ltd. (Milwaukee, WI). Diethylenetriamine (DET) was purchased from Tokyo Kasei Kogyo (Tokyo, Japan) and distilled over CaH_2 under reduced pressure. DMF was dehydrated using activated molecular sieves (4A) and distilled under reduced pressure. PEG-PAsp(DET) block copolymer (PEG: 12,000 g/mol, polymerization degree of PAsp(DET) segment: 68) was synthesized as previously reported [11]. Alexa Fluor 680 (Alexa680) succinimidyl ester was a product of Invitrogen (Carlsbad, CA). A Micro BCA protein assay reagent kit was purchased from Pierce (Rockford, IL). The Luciferase assay kit was a product of Promega (Madison, WI). Plasmid pCAcc+Luc coding for firefly luciferase under the control of the CAG promoter was provided by RIKEN Gene Bank (Tsukuba, Japan), amplified in competent DH5a *Escherichia coli*, and then purified using a HiSpeed Plasmid MaxiKit purchased from Qiagen Sciences (Germantown, MD). pDNA encoding for a soluble form of VEGF receptor-1 (sFlt-1) was prepared as previously reported [16].

2.2. Animals

Balb/c mice (female, 8 weeks old) and balb/c nude mice (female, 5 weeks old) were purchased from Charles River Laboratories (Tokyo, Japan). All animals were treated in accordance with the guideline of the Animal Ethics Committee of The University of Tokyo.

2.3. Synthesis of α-methoxy-ω-cholesteryl carbamate poly(ethylene glycol)-block-poly{N-[N-(2-aminoethyl)-2-aminoethyl]aspartamide} [PEG-PAsp(DET)]

PEG-*b*-poly(β-benzyl L-aspartate) (PEG-PBLA) (PEG: 12,000 g/mol, polymerization degree of PBLA segment: 68) was prepared as previously reported [11]. PEG-PBLA (210 mg) was dissolved in CH_2Cl_2 (4 mL), followed by the addition of 11 v/v% TEA/CH_2Cl_2 (200 μL) and cholesterol chloroformate (344 mg) in CH_2Cl_2 (1 mL) at 0 °C. The reaction mixture was stirred at room temperature for 24 h. The reactant polymer was isolated by precipitation into diethylether and lyophilized from benzene, to obtain PEG-PBLA-Chole (197 mg). PEG-PBLA-Chole (100 mg) was dissolved in DMF (4 mL), followed by reaction with DET (50 equiv. to benzyl group of PBLA segment, 1.43 g) at 40 °C. After 1 h, the reactant mixture was slowly added to a 20% acetic acid (13.8 mL) solution, and subsequently dialyzed against 0.01 N HCl and finally distilled water. The final solution was lyophilized to obtain PEG-PAsp (DET)-Chole (98 mg).

The ^{1}H NMR spectrum of each polymer was obtained with an EX300 spectrometer (JEOL, Tokyo, Japan). Chemical sifts were reported in ppm relative to the residual protonated solvent peak.

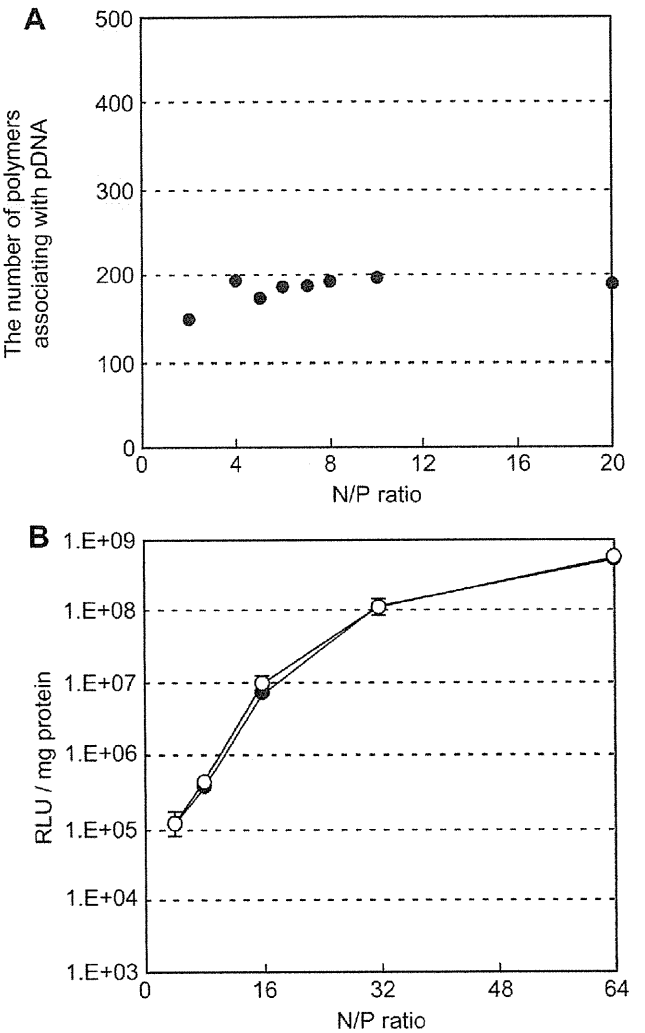

Fig. 1. (A) The number of PEG-PAsp(DET-Alexa680) block copolymers associating with a pDNA. (B) Transfection efficiency of PEG-PAsp(DET) polyplex micelles. Closed circles: addition of polyplex micelle solutions prepared at various N/P ratios into the cell culture medium. Open circles: addition of polyplex micelle solutions prepared at a constant N/P value of 4, with separate addition of PEG-PAsp(DET) free polymer solution into the cell culture medium to obtain the same N/P values shown in the experiment with open circles.

2.4. Introduction of Alexa680 into block copolymers

Alexa680 was introduced into the side chains of both PEG-PAsp(DET) and PEG-PAsp(DET)-Chole polymers. The typical synthetic procedure of PEG-PAsp(DET-Alexa680) is described as follows: Alexa680 succinimidyl ester (1 mg) in 100 μL of DMF was added to PEG-PAsp(DET) (30 mg) in 1.5 mL of 0.1 N $NaHCO_3$ (pH 9.3) and stirred at 4 °C for 1 h. The reacted polymer was purified by dialysis against distilled water and lyophilized to obtain PEG-PAsp(DET-Alexa680) (22 mg). Introduction of Alexa680 into PEG-PAsp(DET)-Chole was completed similarly using Alexa680 succinimidyl ester (1 mg) and PEG-PAsp(DET)-Chole (30 mg) to obtain PEG-PAsp(DET-Alexa680)-Chole (23 mg). The number of Alexa680 introduced into the strand of

PEG-PAsp(DET) and PEG-PAsp(DET)-Chole was estimated to be 0.6 and 0.7, respectively, using a spectrofluorometer (ND-3300, NanoDrop, Wilmington, DE).

2.5. Preparation of polyplex micelles

Each block copolymer and pDNA was dissolved separately in 10 mM Tris–HCl buffer (pH 7.4) or 10 mM Hepes buffer (pH 7.3). Polymer solutions of various concentrations were added to a two-fold excess volume of pDNA solution to form polyplex micelles with different compositions. The final pDNA concentration was adjusted to 33.3 μg/mL for *in vitro* experiments and 100 μg/mL for *in vivo* experiments and micelle solutions were stored at 4 °C overnight prior to use. The N/P ratio was defined as the residual molar ratio of the amino groups of PAsp(DET) units to the phosphate groups of pDNA. The N^+/P ratio was defined as the molar ratio of protonated amino groups of PAsp(DET) units to the phosphate groups of pDNA.

2.6. Ultracentrifugation

In order to evaluate the amount of free polymer in the polyplex micelle solution, ultracentrifugation analysis of polyplex micelles, composed of Alexa680-labeled block copolymers and pDNA, was carried out by a Beckman XL-I ultracentrifuge (Beckman Coulter, Inc., Fullerton, CA) using an An-60 Ti 4-hole rotor and standard double-sectors (Epon centerpieces) equipped with quartz windows. The concentration of polyplex micelle solutions prepared at various N/P ratios were adjusted to 33.3 μg pDNA/mL in 10 mM Hepes buffer (pH 7.3). Sedimentation of polyplex micelles was confirmed by UV absorbance measurement at 260 nm, while that of Alexa680-labeled polymers was confirmed by visible absorbance at 680 nm. Polyplex micelle solutions prepared at various N/P ratios were ultracentrifuged at 49,000 g for 1 h in order to sediment only the polyplex micelles. The concentration of free polymers contained in the supernatant was calculated using a calibration curve prepared from Alexa680-labeled polymer solutions. The number of block copolymers associating with pDNA was then estimated from the calculated concentration of free polymers.

2.7. Dynamic light scattering (DLS) measurement

The size of the polyplex micelles was evaluated by DLS using Nano ZS (ZEN3600, Malvern Instruments, Ltd., UK). A He–Ne ion laser (633 nm) was used as the incident beam. The concentration of polyplex micelle solutions prepared at various N/P ratios were adjusted to 33.3 μg pDNA/mL in 10 mM Tris–HCl buffer (pH 7.4). Light scattering data was obtained at a detection angle of 173° and a temperature of 37 °C and was subsequently analyzed by the cumulant method to obtain the hydrodynamic diameters and polydispersity indices (PDI) (μ/T^2) of the micelles.

2.8. Stability of polyplex micelles against bovine serum albumin (BSA)

Polyplex micelle solution (33.3 μg pDNA/mL) prepared at N/P ratio = 2 was adjusted to 10 μg pDNA/mL in 10 mM Tris–HCl buffer (pH 7.4) with 150 mM NaCl and 0.1 mg/mL BSA. DLS measurements of the polyplex micelle solution were then carried out every 30 min at 37 °C using Nano ZS.

2.9. In vitro transfection

Huh-7 and HeLa cells were separately seeded onto 24-well culture plates (10,000 cells/well) and incubated overnight in 500 μL of Dulbecco's Modified Eagle Medium (DMEM) containing 10% fetal bovine serum (FBS). The medium was exchanged and the pDNA micelle solutions (33.3 μg pDNA/mL) prepared at various N/P ratios were applied to each well at the desired concentrations. The amount of micelle solution added was as follows: 30 μL for 2 μg pDNA/mL, 10 μL for 2/3 μg pDNA/mL, or 3.3 μL for 2/9 μg pDNA/mL. For experiments shown in Fig. 1B (open circles), polymer solution was added to cultured Huh-7 cells simultaneously with PEG-PAsp(DET) micelle (N/P = 4), in order to elucidate the effect of free polymer on transfection efficiency. After 24-h incubation, the medium was replaced with 500 μL of fresh medium, followed by 24-h further incubation. Luciferase gene expression was then evaluated based on photoluminescence intensity using the Luciferase assay kit and a Luminometer (Lumat LB9507, Berthold Technologies, Bad Wildbad, Germany). The amount of protein in each well was concomitantly determined using a Micro BCA protein assay kit. One nanogram of luciferase corresponded to 9.1×10^7 RLU in our experiments according to a standard curve calibrated with recombinant luciferase (QuantiLum, Promega).

2.10. Cytotoxicity of polyplex micelles

Huh-7 and HeLa cells were separately seeded onto 96-well culture plates (2500 cells/well) and incubated overnight in 100 μL of DMEM containing 10% FBS. After the medium was replaced with fresh medium, 7.5 μL of polyplex micelle solution (33.3 μg pDNA/mL) prepared at various N/P ratios was applied to each well (0.25 μg pDNA/well). After 24-h incubation, the medium was replaced with 100 μL of fresh medium, followed by 24-h incubation. Cell viability was evaluated using the MTT assay. Briefly, 20 μL of MTT solution (5 mg/mL in PBS) was added to each well, followed by 3-h incubation at 37 °C. Then, 100 μL of sodium dodecyl sulfate (SDS) solution (20 w/v% in PBS) was added to dissolve the formed formazan. After 15-min incubation at room temperature, the absorbance from each well was measured at 570 nm. Results were expressed as percentage relative to non-treated controls.

2.11. Cellular uptake of polymers and pDNA

Polyplex micelles were prepared with non-labeled polymer and Cy3-labeled pDNA (Fig. 8A), or with Alexa680-labeled polymer and non-labeled pDNA (Fig. 8B) for these experiments. pDNA was labeled with Cy3 using a Label IT Nucleic Acid Labeling Kit (Mirus, Madison, WI) according to the manufacturer's protocol. Huh-7 cells were seeded on 24-well culture plates (10,000 cells/well) and incubated overnight in 500 μL of DMEM containing 10% FBS. The medium was replaced with fresh medium and then 30 μL of polyplex micelle solution (33.3 μg pDNA/mL) was applied to each well. After 24-h incubation, the medium was removed and the cells were washed 3 times with PBS and detached with trypsin. Harvested cells were re-suspended in PBS and analyzed using the flow cytometer (BD LSR II, BD, Franklin Lakes, NJ).

2.12. Confocal laser scanning microscope (CLSM) observation

pDNA was labeled with Cy5 according to manufacturer's protocol using a Label IT Nucleic Acid Labeling Kit. Huh-7 cells (30,000) were seeded on a 35-mm glass base dish (Iwaki, Tokyo, Japan) and incubated overnight in 1.5 mL of DMEM containing 10% FBS. After the medium was exchanged, 90 μL of polyplex micelle solution (33.3 μg pDNA/mL) was applied to each sample. After 24-h incubation, the medium was removed and the cells were washed three times with PBS. The intracellular distribution of the polyplex micelles was observed by CLSM after staining acidic late endosomes/lysosomes with Lyso Tracker Green (Molecular Probes, Eugene, OR), and nuclei with Hoechst 33342 (Dojindo Laboratories, Kumamoto, Japan). CLSM observation was performed using an LSM 510 (Carl Zeiss, Oberlochen, Germany) equipped with a 63× objective (C-Apochromat, Carl Zeiss) at the excitation wavelengths of 488 nm (Ar laser) for Lyso Tracker Green, 633 nm (He–Ne laser) for Cy5, and 710 nm (MaiTai laser, 2 photon excitation; Spectra-Physics, Mountain View, CA) for Hoechst 33342. To evaluate the endosomal escaping behavior of polyplex micelles, the rate of colocalization of Cy5-labeled pDNA with Lyso Tracker Green was quantified [17]. Colocalization was quantified as follows:

$$\text{Amount of colocalization}(\%) = \text{Cy5 pixels}_{\text{colocalization}}/\text{Cy5 pixels}_{\text{total}} \times 100$$

where $\text{Cy5 pixels}_{\text{colocalization}}$ represents the number of Cy5 pixels colocalizing with Lyso Tracker Green in the cell, and $\text{Cy5 pixels}_{\text{total}}$ represents the number of all the Cy5 pixels in the cell.

2.13. Fluorescence correlation spectroscopy (FCS) measurement

PEG-PAsp(DET-Alexa680)-Chole free polymer, polyplex micelles composed of PEG-PAsp(DET-Alexa680)-Chole and pDNA, and polyplex micelles composed of PEG-PAsp(DET) and Cy5-labeled pDNA, were used in this experiment. Block copolymers and polyplex micelles (N/P = 8) were adjusted to a polymer concentration of 187 μg/mL (33.3 μg pDNA/mL) in 10 mM Hepes buffer (pH 7.3), and then diluted to a concentration of 18.7 μg/mL using 10 mM Hepes buffer (pH 7.3) (Fig. 10A) or 10 mM MES buffer (pH 5.5) (Fig. 10B), or 2.08 μg/mL using 10 mM Hepes buffer (pH 7.3) (Fig. 10A). FCS measurements were carried out using an LSM 510 (Carl Zeiss) equipped with a 40× objective (C-Apochromat, Carl Zeiss) and the ConfoCor3 module. Excitation of Alexa680 and Cy5 was achieved with a He–Ne laser (633 nm). The relative diffusion times of polymer and micelles (Fig. 10A) were determined using PEG-PAsp(DET-Alexa680)-Chole solution and its polyplex micelle solution, respectively. Furthermore, the percentage of polymers associating with pDNA in the micelle solution was calculated as follows:

$$\text{Percentage of polymers associating with pDNA} = \left[\text{Nfp}_{\text{PEG-PAsp(DET-Alexa680)-Chole}} - \left(\text{Nfp}_{\text{PEG-PAsp(DET-Alexa680)-Chole/pDNA}} - \text{Nfp}_{\text{PEG-Pasp(DET)-Chole/Cy5-pDNA}}\right)\right] / \text{Nfp}_{\text{PEG-PAsp(DET-Alexa680)-Chole}} \times 100$$

where $\text{Nfp}_{\text{PEG-PAsp(DET-Alexa680)-Chole}}$ represents the number of fluorescent particles (free polymers) in PEG-PAsp(DET-Alexa680)-Chole solution, $\text{Nfp}_{\text{PEG-PAsp(DET-Alexa680)-Chole/pDNA}}$ represents the number of fluorescent species (free polymers and micelles) in PEG-PAsp(DET-Alexa680)/pDNA micelle solution, and $\text{Nfp}_{\text{PEG-Pasp(DET)-Chole/Cy5-pDNA}}$ represents the number of fluorescent species (micelles) in PEG-PAsp (DET)-Chole/Cy5-pDNA micelle solution.

2.14. Stability of polyplex micelles in the blood stream

Polyplex micelles (N/P = 8) incorporating Cy5-labeled pDNA (100 μg pDNA/mL, 200 μL) in 10 mM Hepes buffer (pH 7.3) with 150 mM NaCl were intravenously injected into the tail vein of balb/c mice at a dose of 20 μg pDNA/mouse. Blood

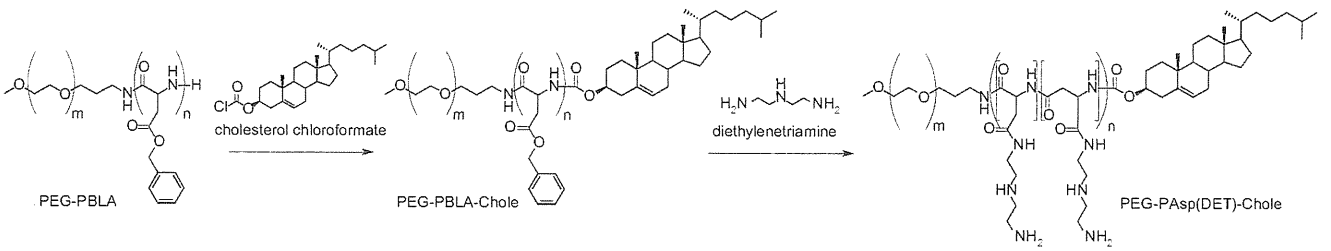

Scheme 1. Synthesis of PEG-PAsp(DET)-Chole block copolymer.

was collected from the postcaval vein under anesthesia at appointed times after injection, followed by centrifugation to obtain the plasma. Two microliters of 10× trypsin-EDTA were added to 20 μL of the obtained plasma and incubated at 37 °C overnight. The fluorescence intensity of the sample solution was measured using a spectrofluorometer (ND-3300, NanoDrop). The injected dose (%) was calculated using a standard curve.

2.15. Anti-tumor activity assay

Balb/c nude mice were inoculated subcutaneously with human pancreatic adenocarcinoma BxPC3 cells (5×10^6 cells in 100 μL of PBS). Tumors were allowed to grow for 2–3 weeks to reach proliferative phase (approximately 45 mm^3). Subsequently, polyplex micelles loading pDNA encoding sFlt-1 (20 μg pDNA/mouse) in 10 mM Hepes buffer (pH 7.3) with 150 mM NaCl were injected into the tail vein 3 times at 4-day intervals. Tumor volume (V) was calculated as the following equation:

$$V = a \times b^2/2$$

where a and b denote the long and short diameters of the tumor tissue, respectively.

3. Results

3.1. Ultracentrifugation analysis of PEG-PAsp(DET) polyplex micelles

The amount of free block copolymer in PEG-PAsp(DET) micelle solutions was quantified by ultracentrifugation analysis of polyplex micelles prepared with fluorescent-labeled block copolymer [PEG-PAsp(DET-Alexa680)]. Polyplex micelles were confirmed to precipitate after 1 h of ultracentrifugation at 49,000 g, whereas free block copolymers could not sediment (data not shown). Thus, the amount of free block copolymers was estimated by visible absorbance at 680 nm. Fig. 1A shows the number of block copolymers associating with a pDNA in the polyplex micelle solution prepared at each N/P ratio. Note that a stoichiometric charge ratio of PEG-

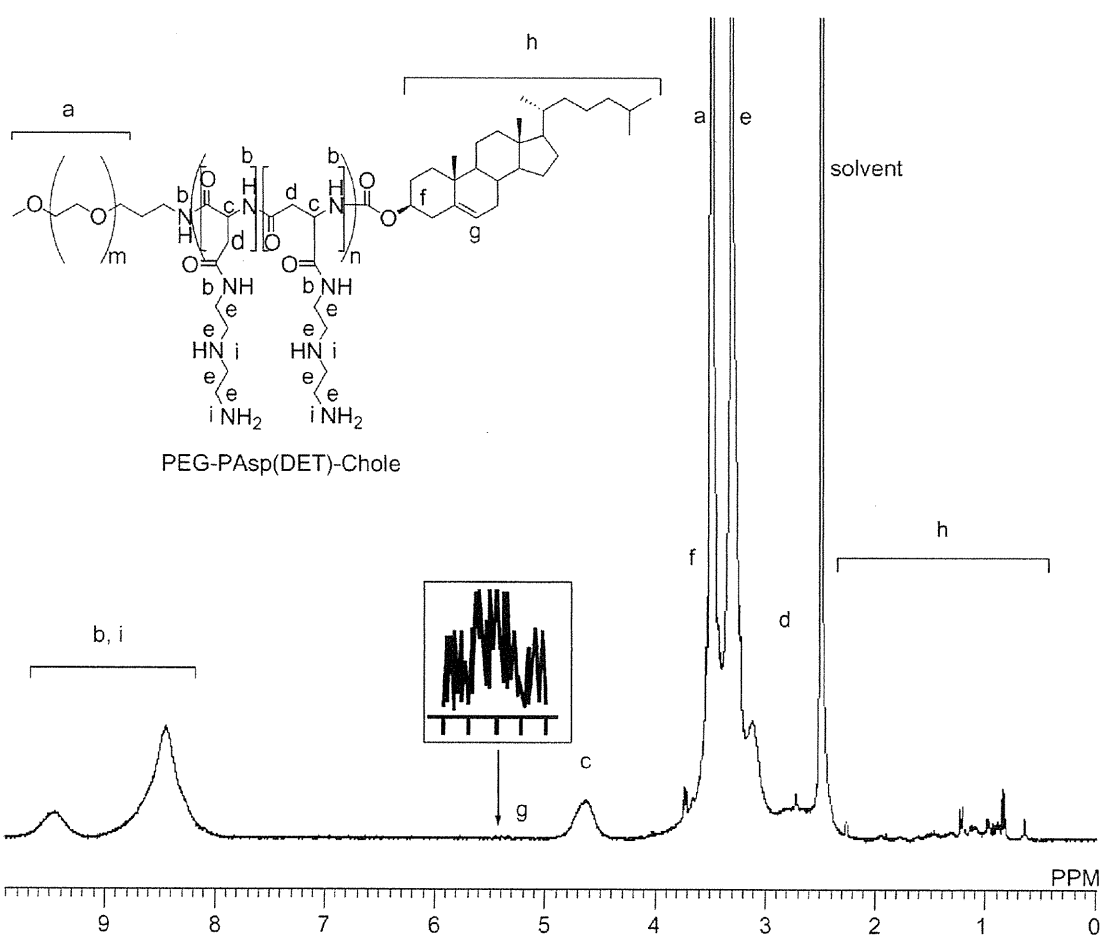

Fig. 2. ^{1}H NMR spectrum of PEG-PAsp(DET)-Chole block copolymer in DMSO at 25 °C.

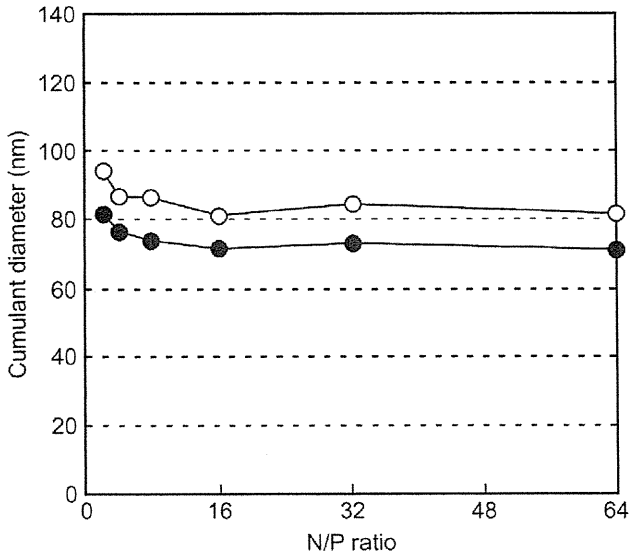

Fig. 3. Cumulant diameters of PEG-PAsp(DET) (closed circles) and PEG-PAsp(DET)-Chole (open circles) polyplex micelles.

PAsp(DET) micelle should be N/P = 2 ($N^+/P = 1$) because half of the amino groups in PAsp(DET) are protonated at pH 7.4 [11]. The number of block copolymers associating with a pDNA at N/P = 2 and at N/P ≥ 4 ($N^+/P \geq 2$) was estimated to be 150 and approximately 190, respectively by the results obtained by ultracentrifugation experiments. The theoretical number of block copolymers associating with a pDNA at stoichiometric charge ratio was calculated to be 189 based on complete neutralization of PAsp(DET) with a polymerization degree = 68 and pDNA with 6411 bp long. This result indicated that PEG-PAsp(DET)/pDNA polyplex micelles at N/P ≥ 4 ($N^+/P \geq 2$) were formed at polymer/pDNA charge ratio = 1/1 (polymer/pDNA molar ratio = 190/1), and that the block copolymers present in solution in excess of that ratio should exist as free polymers at this concentration.

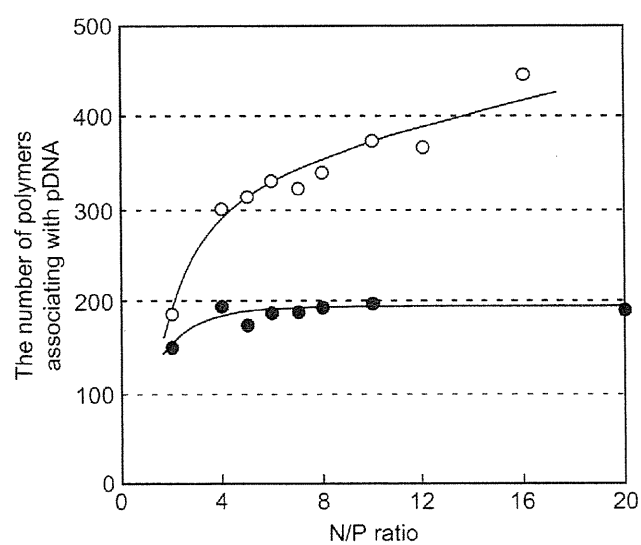

Fig. 4. The number of PEG-PAsp(DET-Alexa680) (closed circles) and PEG-PAsp(DET-Alexa680)-Chole (open circles) block copolymers associating with a pDNA.

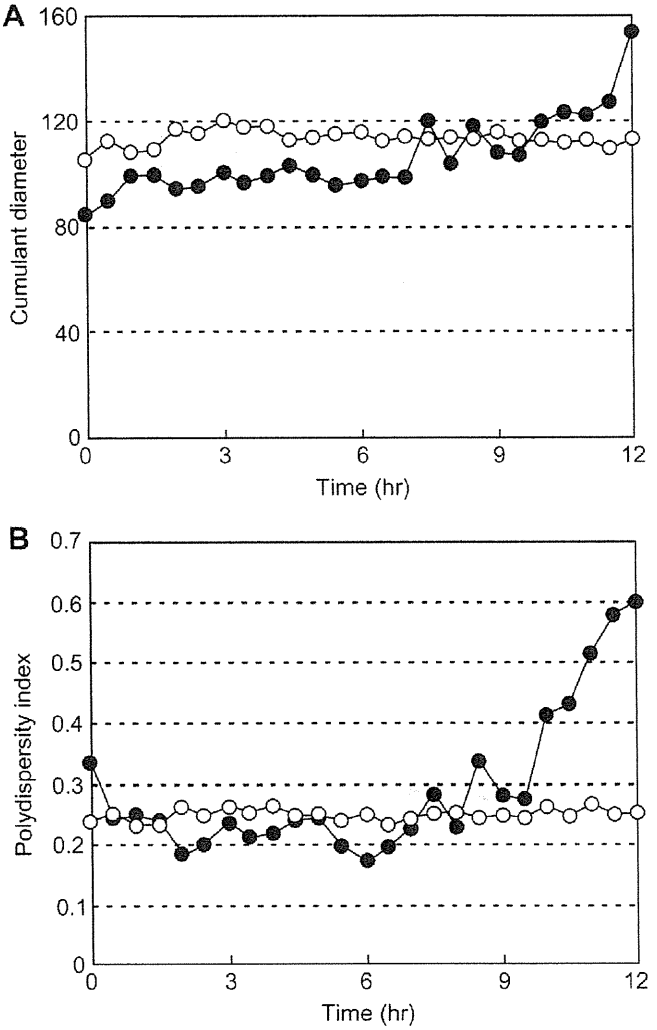

Fig. 5. Time-dependent change of cumulant diameters (A) and polydispersity index (PDI: μ/Γ^2) (B) of polyplex micelles (N/P = 2) in the presence of bovine serum albumin (0.1 mg/mL). Closed circles: PEG-PAsp(DET) polyplex micelles. Open circles: PEG-PAsp (DET)-Chole polyplex micelles.

3.2. In vitro transfection efficiency of PEG-PAsp(DET) polyplex micelles

In order to confirm the effects of free polymer on *in vitro* transfection, we evaluated the transfection efficiency of PEG-PAsp (DET) micelles in Huh-7 cells under the following conditions: (i) polyplex micelles prepared at each N/P ratio; (ii) polyplex micelles prepared with PEG-PAsp(DET) at N/P = 4 with addition of free polymer to achieve the same polymer concentration achieved at each N/P ratio used in condition (i). Under the conventional transfection conditions used in (i) above, the transfection efficiency increased with N/P ratio as previously reported [11]. Surprisingly, the profile of transfection efficiency under the condition (ii) showed the same behavior as that under the condition (i) with the addition of free polymer as shown in Fig. 1B. These results imply that increased transfection efficiency of PEG-PAsp(DET) micelles prepared at high N/P ratios might involve the effect of non-associating polymers with pDNA in the culture medium.

3.3. Synthesis of PEG-PAsp(DET)-Chole block copolymer

PEG-PAsp(DET)-Chole was synthesized using PEG-PBLA (PEG: 12,000 g/mol, polymerization degree of PBLA segment: 68) [11] as a starting material (Scheme 1). Addition of excessive cholesterol chloroformate and TEA to PEG-PBLA, which possessed a primary amino group in the terminus of PBLA, in CH_2Cl_2 afforded PEG-PBLA-Chole with ω-terminus of cholesterol. Conversion of PBLA segment into PAsp(DET) segment was achieved by aminolysis reaction [18]. Introduction rates of cholesterol and ethanediamine were determined by ^1H NMR analysis (Fig. 2) based on the peak intensity ratio of the methylene protons of PEG (OCH_2CH_2, δ = 3.6 ppm) to the vinyl proton of cholesterol ($C{=}CHCH_2$, δ = 5.4 ppm), or to the methylene protons of DET ($NHCH_2CH_2NHCH_2CH_2NH_2$, δ = 3.1–3.5 ppm), respectively. Cholesterol introduction and the aminolysis reaction were confirmed to proceed quantitatively.

3.4. Formation of PEG-PAsp(DET)-Chole polyplex micelles

Agarose gel electrophoresis showed that free pDNA was not detected in both PEG-PAsp(DET) and PEG-PAsp(DET)-Chole micelles at N/P > 1.75 ($N^+/P > 0.875$) (data not shown), confirming that all of the pDNA were entrapped in polyplex micelles. Complex formation of pDNA with PEG-PAsp(DET) at pH 7.4 was previously reported to reach completion at N/P ≈ 2 ($N^+/P \approx 1$) [11,19], which is consistent with the result obtained in this work. Complex formation was not hindered by cholesterol introduction into the PAsp(DET) segment of the block copolymer as the N^+/P for complete pDNA entrapment did not change compared to the parent polymer. The size of the polyplex micelles was evaluated by DLS (Fig. 3). The cumulant diameters of polyplex micelles prepared with both block copolymers were found to be approximately 70–80 nm by DLS measurement.

3.5. Ultracentrifugation analysis of PEG-PAsp(DET)-Chole polyplex micelles

The amount of free polymer in PEG-PAsp(DET)-Chole micelle solution was also quantified by the same method as described for micelles prepared with PEG-PAsp(DET). As shown in Fig. 4, the number of polymers associating with a pDNA at N/P = 2 ($N^+/P = 1$) was approximately 190, which corresponds to the stoichiometric value. However, at N/P > 2 ($N^+/P > 1$), micelles formed with PEG-PAsp(DET)-Chole exhibited an increased number of polymers in the polyplex (in excess of the stoichiometric charge ratio), whereas micelles prepared with PEG-PAsp(DET) showed a constant number of associated polymers.

3.6. Stability of polyplex micelles against bovine serum albumin (BSA)

PEG-PAsp(DET) micelles have high transfection ability with low cytotoxicity at high N/P ratios, however, they are unstable and easily decondensed in the medium containing serum [20], probably

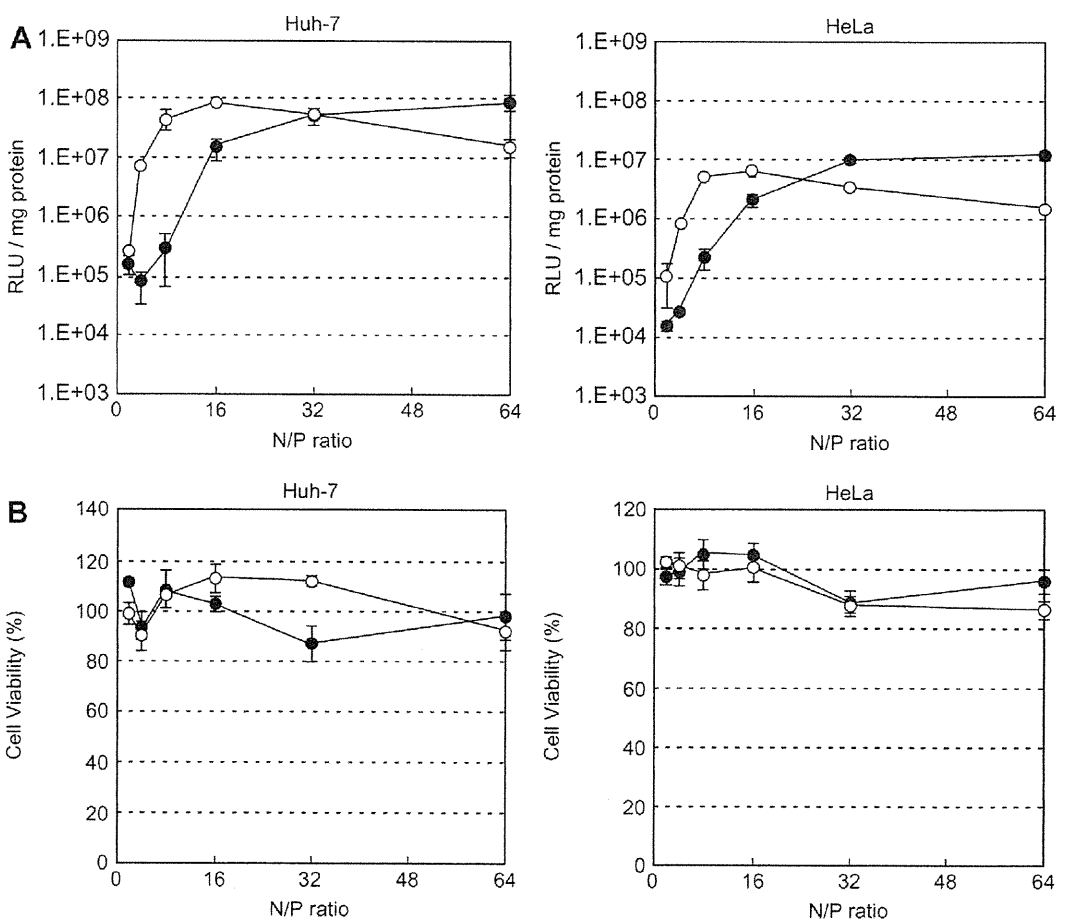

Fig. 6. Transfection efficiency (A) and cytotoxicity (B) of polyplex micelles prepared at various N/P ratios against Huh-7 cells and HeLa cells. Closed circles: PEG-PAsp(DET) polyplex micelles. Open circles: PEG-PAsp(DET)-Chole polyplex micelles. Error bars in the graph represent SEM, n = 4.

due to the weak association power of PAsp(DET) segment with pDNA. Therefore, the stability of polyplex micelles containing cholesterol was compared to micelles without cholesterol by monitoring the time-dependent change of cumulant diameter and PDI in the presence of BSA (Fig. 5). After adding BSA (0.1 mg/mL) to polyplex micelle solution (prepared at N/P = 2), the cumulant diameter and PDI were measured every 30 min. PEG-PAsp(DET)-Chole micelles maintained their initial size and PDI for 12 h (Fig. 5A). On the other hand, the size and PDI of micelles prepared with PEG-PAsp(DET) remained constant for only ~6 h and then gradually increased, and monodispersity was not maintained (Fig. 5B). These results imply that cholesterol introduction resulted in increased stability of polyplex micelles in BSA solution.

3.7. *In vitro transfection efficiency and cytotoxicity of polyplex micelles*

The *in vitro* transfection efficiency of PEG-PAsp(DET) and PEG-PAsp(DET)-Chole micelles prepared at various N/P ratios was evaluated against Huh-7 and HeLa cells by the luciferase assay (Fig. 6A). Transfection efficiencies of PEG-PAsp(DET) micelles increased with N/P ratio, and reached a maximum at N/P 32–64. However, PEG-PAsp(DET)-Chole micelles showed the highest transfection efficiencies at N/P = 8–16, with maximum transfection levels comparable to PEG-PAsp(DET). Cholesterol introduction clearly enhanced transfection efficiency at lower N/P ratios, especially at N/P 4 and 8. Fig. 6B shows the results of cytotoxicity analysis performed under the same condition as the luciferase assay. Increased cytotoxicity as a result of cholesteryl introduction was not detected in Huh-7 and HeLa cells.

3.8. *Effect of pDNA concentration on transfection efficiency*

All transfection experiments in the preceding section were carried out at a constant pDNA concentration of 2 μg pDNA/mL (1 μg pDNA/well, 24-well plate) (Fig. 6). Here additional transfection experiments were repeated against Huh-7 cells at the diluted concentration of 2, 2/3, and 2/9 μg pDNA/mL in order to confirm the influence of dilution (Fig. 7). The transfection efficiency of PEG-PAsp(DET) micelles markedly decreased with reduced pDNA concentration (Fig. 7A), while of the transfection ability of PEG-PAsp(DET)-Chole micelles was maintained without a severe decrease (Fig. 7B). PEG-PAsp(DET) micelles at N/P = 16 showed approximately 1/1000 of transfection efficiency in response to the concentration change from 2 μg to 2/9 μg pDNA/mL. In contrast, the decrease in the transfection with PEG-PAsp(DET)-Chole micelles was less than 1/10. Thus, transfection efficiency of PEG-PAsp(DET)-Chole micelles was confirmed to be more tolerable in dilution compared to PEG-PAsp(DET) micelles, suggesting their feasibility for *in vivo* gene delivery, which requires high transfection ability under highly diluted conditions.

3.9. *Cellular uptake of micelles*

Flow cytometric analysis was used to quantify the cellular uptake of micelles with respect to pDNA (Fig. 8A) and polymer (Fig. 8B) by using Cy3-labeled pDNA and Alexa680-labeled polymer, respectively. PEG-PAsp(DET)-Chole micelles showed higher pDNA uptake than PEG-PAsp(DET) micelles at both N/P = 8 and 16 (Fig. 8A). Cholesterol introduction enhanced the stability of polyplex micelles against BSA (shown in Fig. 5), thus, PEG-PAsp (DET)-Chole micelles likely maintained their structures without dissociation or aggregation in the cell culture medium, which likely increased the uptake of pDNA. The cellular uptake of polymer was also higher for PEG-PAsp(DET)-Chole than PEG-PAsp(DET) (Fig. 8B). PEG-PAsp(DET)-Chole polymers might be more effectively internalized into the cells due to their strong association power towards pDNA.

3.10. *CLSM observation and evaluation of endosomal escape*

The intracellular distribution of polyplex micelles was investigated by CLSM using Cy5-labeled pDNA (red) incorporated micelles (Fig. 9A). Lyso Tracker Green (green) and Hoechst 33342 (blue) were used to label late endosomes/lysosomes and nuclei, respectively. The amount of Cy5-pDNA observed in the cells was much higher for PEG-PAsp(DET)-Chole micelles than PEG-PAsp (DET) micelles at both N/P = 8 and 16, which was consistent with the results obtained by flow cytometric analysis (Fig. 8A). Colocalization of pDNA with the late endosomes/lysosomes was

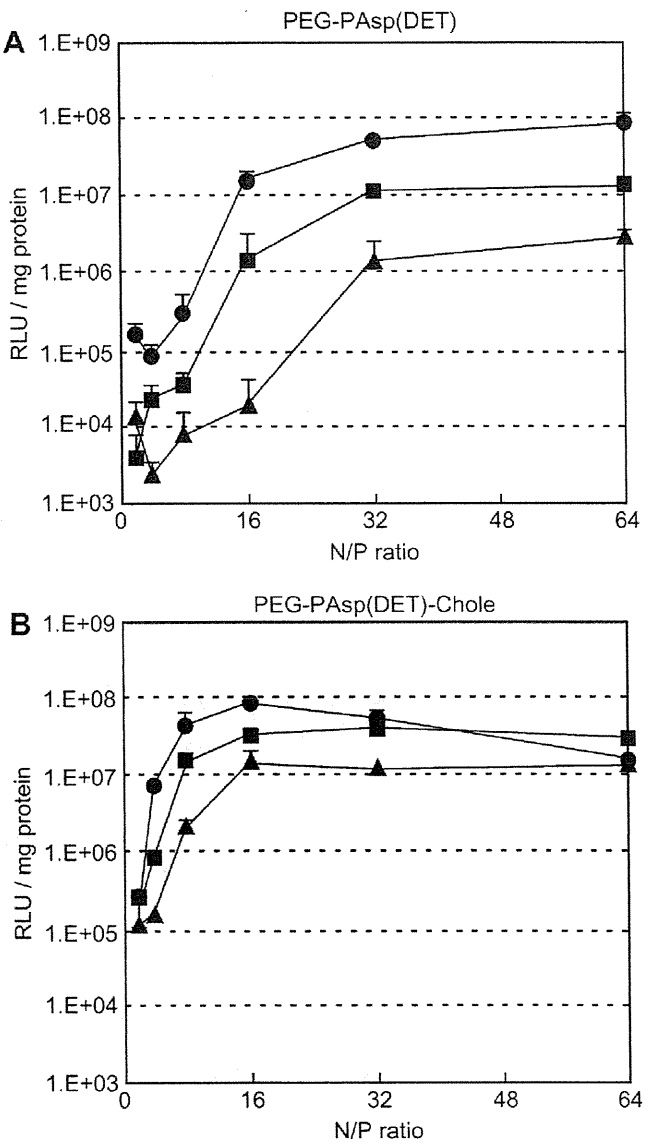

Fig. 7. Effect of pDNA concentration on transfection efficiency of PEG-PAsp(DET) (A) and PEG-PAsp(DET)-Chole (B) polyplex micelles against Huh-7 cells. Closed circles, squares, and triangles represent 2 μg/mL, 2/3 μg/mL, and 2/9 μg/mL of pDNA concentration in the culture medium, respectively. Error bars in the graph represent SEM, $n = 4$.

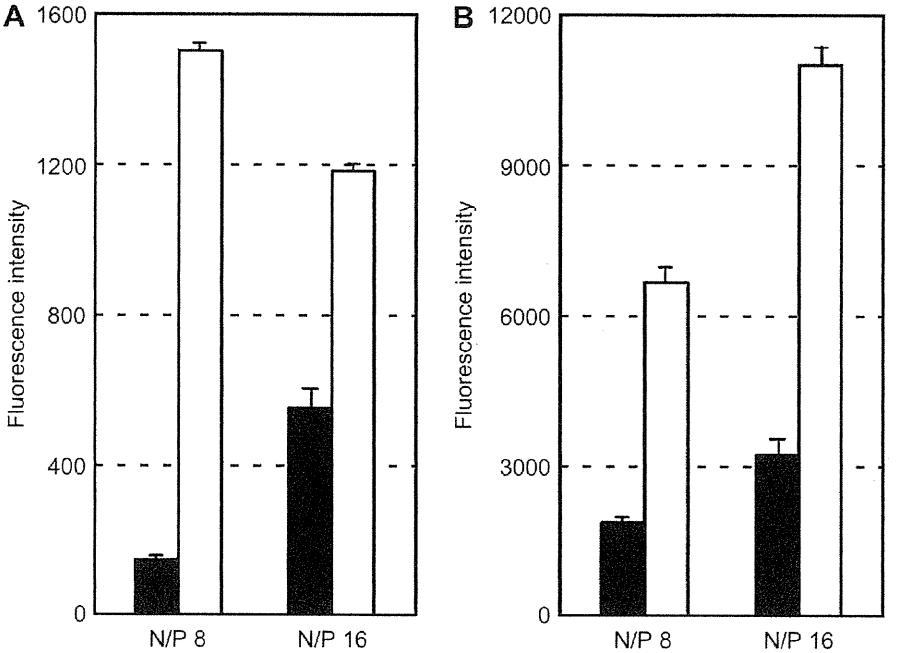

Fig. 8. Cellular uptake of Cy3-labeled pDNA (A) and Alexa680-labeled polymers (B). Closed bars: PEG-PAsp(DET) polyplex micelles. Open bars: PEG-PAsp(DET)-Chole polyplex micelles. Error bars in the graph represent SEM, $n = 4$.

quantified and shown in Fig. 9B. At N/P = 8, more than 80% of pDNA in PEG-PAsp(DET) micelles was localized in the late endosomes/lysosomes, while only 20% of that in PEG-PAsp(DET)-Chole micelles was localized there. These results revealed that PEG-PAsp(DET)-Chole micelles internalized into the cells could achieve effective endosomal escape. Note that increasing N/P ratio appreciably decreased the endosomal/lysosomal entrapment of PEG-PAsp(DET) micelles from more than 80% to less than 60%, consistent with the result of the transfection efficiency (Fig. 6).

3.11. FCS measurement

FCS analysis was performed in order to estimate a change in the association state of polyplex micelles with respect to dilution and pH (Fig. 10). At pH 7.3, the relative diffusion time of PEG-PAsp (DET)-Chole micelle solution was approximately 8-fold higher than that of PEG-PAsp(DET)-Chole polymer solution, and the diffusion time was not significantly changed by 9-fold dilution (Fig. 10A). These results suggest that the association state of PEG-PAsp(DET)-Chole micelles remains constant in this concentration range, which

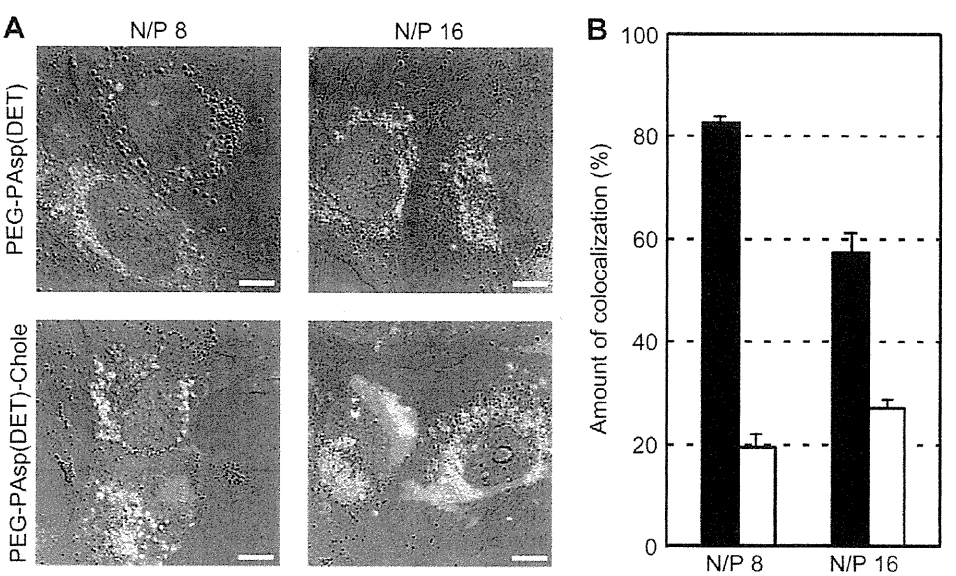

Fig. 9. (A) CLSM observation of the intracellular distribution of polyplex micelles containing Cy5-labeled pDNA (red) with late endosomes/lysosomes (green) and nuclei (blue) stained using Lyso Tracker Green and Hoechst 33342, respectively. Bars represent 10 μm. (B) Quantification of Cy5-labeled pDNA colocalization with Lyso Tracker Green in the Huh-7 cells. Closed bars: PEG-PAsp(DET) polyplex micelles. Open bars: PEG-PAsp(DET)-Chole polyplex micelles. Error bars in the graph represent SEM, $n = 10$.